Research article

Grid-based climate variability analysis of Addis Ababa, Ethiopia

Esubalew Nebebe Mekonnen [a],[*], Aramde Fetene [b], Ephrem Gebremariam [a]

[a] *Computer Aided Design and Geoinformatics, EiABC, Addis Ababa University, Addis Ababa, Ethiopia*
[b] *Environmental Planning and Landscape Design, EiABC, Addis Ababa University, Addis Ababa, Ethiopia*

ARTICLE INFO

ABSTRACT

Climate change is an intricate global environmental concern. However, its impact is more pervasive in developing nations such as Ethiopia. Hence, this manuscript examines temperature variability and the magnitude of change over 38 years in the specific case of Addis Ababa, Ethiopia. Gridded meteorological data consisting of minimum and maximum temperatures on a monthly time scale ranging from 1981 to 2018 was obtained from the National Meteorological Agency of Ethiopia. The coefficient of variation (CV) and standardized anomaly index (SAI) were used to examine the rate and extent of temperature anomalies. Geostatistical models, particularly ordinary kriging, are presented as a means of spatially interpolating temperature data. Modified Mann-Kendall test (MMK), Sen's Slope (SS) estimator, principal component analysis (PCA), and T-test were employed to determine the monthly, annual, and seasonal trends using Geospatial technologies, "R" programming, and statistical software. The findings revealed substantial spatial and temporal variation in Addis Ababa's annual and seasonal maximum and minimum temperatures. The long-term mean annual maximum and minimum temperatures were 25.8 °C and 12.6 °C, respectively. The monthly, annual, and seasonal temperatures accrued significantly except in the months of January and September. It is noteworthy that the decadal maximum temperature has risen by 2.7 °C, while minimum temperatures have displayed comparatively minor fluctuations. Moreover, the findings also exhibited that the average maximum and minimum temperatures increased by 1.88 °C and 1.72 °C, correspondingly and the highest temperature occurred during the spring (*Belg*) season. The first two PCAs (Annual and *Kiremt* Tmax) account for 90% of the temperature variation. In conclusion, the findings underscore the pressing need for the implementation of climate adaptation strategies and policy measures, which can strengthen the city's resilience to imminent climate change-induced hazards. The mounting temperature presents substantial challenges across various sectors within the city, emphasizing the urgency of preemptive actions to mitigate potential repercussions.

1. Introduction

In the current global discourse, climate change has undeniably ascended to a position of paramount importance, eliciting extensive debates and discussions [1]. It is in a state of constant transformation, casting a formidable shadow over the well-being of individuals across the globe. The issue of climate change has risen to an unprecedented level of prominence, fueling impassioned debates on a

---

global scale [1]. In the coming decades, climate change will pose the greatest threat to humankind and global ecosystems [2]. Its transformations are sweeping and profound, imperiling the prosperity of communities worldwide [3,4]. Climate change and its associated variability are no longer isolated phenomena; instead, they have permeated every corner of the planet, leaving no region untouched [5–7]. Human activities have been firmly established as the principal drivers of this on-going global climate shift, leading to extreme fluctuations in daily temperatures and intensified precipitation patterns [8–11]. The primary cause of climate change is human-caused greenhouse gas emissions [12]. There is now unequivocal consensus that human actions have led to significant warming of the atmosphere, the oceans, and the land [6]. Advances in climate science have enabled precise attribution of climate change to greenhouse gas emissions, socioeconomic development, and land use changes [13].

The effects of climate variability extend to shifts in temperature and precipitation patterns, which have been meticulously documented [14]. Over the years, global temperatures have exhibited a discernible shift, rising by 0.74 °C since the pre-industrial era [15]. Since 1850, the last four decades have been successively warmer than any other time [6]. This trajectory aligns closely with predictions from Ref. [16], forecasting a temperature increase of 1.5–2 °C by the end of the twenty-first century. Notably, this rise has been uneven, with temperatures increasing by a mean of 0.37 °C every decade. Consequently, the maximum daily temperature has surged by a cumulative 1.5 °C since the beginning of the 20th century, profoundly affecting various aspects of human existence, including livelihoods, well-being, and socioeconomic conditions [17,18]. The benefit of stabilizing global warming to no more than 1.5 °C above the preindustrial period will outweigh the negative consequences [19].

However, there exists a substantial knowledge gap in understanding the localized and regional repercussions of climate change, particularly in vulnerable regions like Africa. Despite facing heightened exposure to climate change, Africa exhibits limited capacity for adaptation [20–23], partly due to a dearth of climate literacy [13]. This vulnerability is further exacerbated in developing nations, especially within sub-Saharan Africa [24,25], disproportionately affecting low-income countries in tropical and subtropical regions [26–28]. Specific studies have pointed to temperature increases in countries such as Ethiopia, Kenya, and Tanzania [29]. Ethiopia, in particular, stands out as highly susceptible to climate change [13,30], ranking among the most vulnerable nations globally [31,32]. However, the true impact at the local scale remains poorly understood [23], even though climate variability in Ethiopia is linked to phenomena such as El Niño Southern Oscillation (ENSO) and anthropogenic activity [33,34]. To address this, a comprehensive analysis of temperature trends is crucial for assessing the impact on Ethiopia, particularly in regions like the Gurage Zone and West Shewa [35,36]. Recent findings have highlighted that between 1985 and 2018, the average annual maximum temperature in Ethiopia rose significantly [7].

Over fifty percent of the global population lives in urban areas [37], which confront unique challenges arising from climate change, especially in developing regions like Africa [38]. Cities are highly susceptible to the adverse effects of climate extremes such as
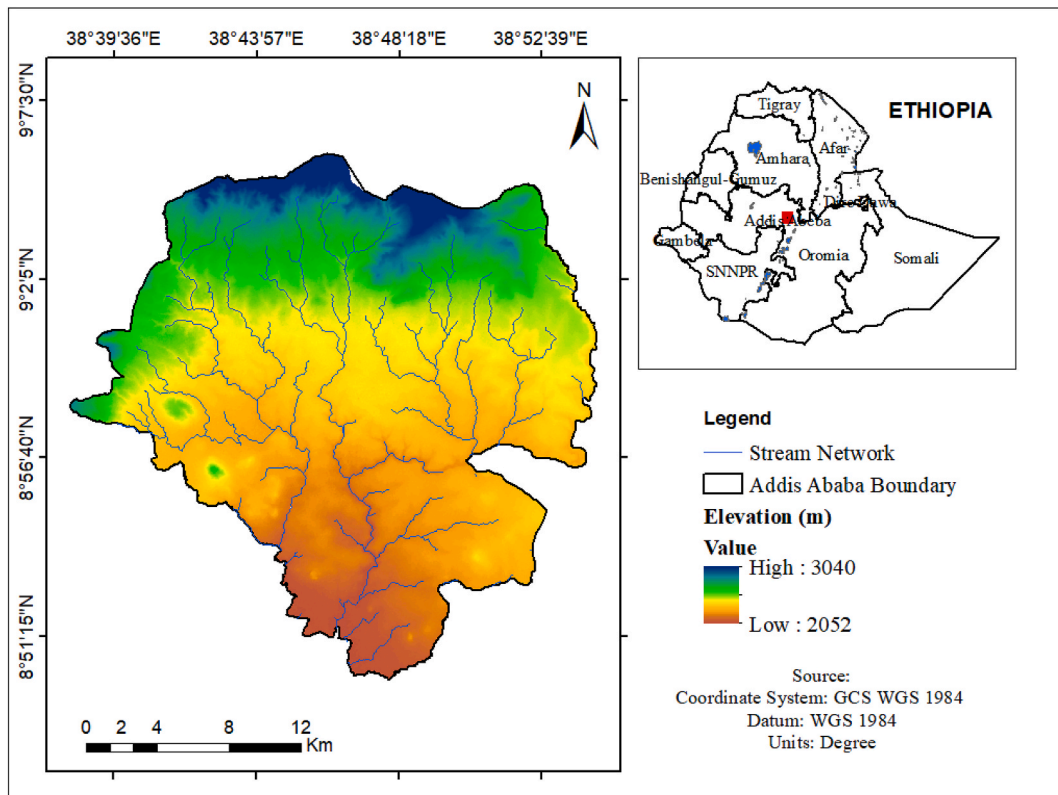

Fig. 1. Study area map.

flooding and increased air temperatures, which threaten livelihoods, damage infrastructure, impact public health, and influence economies and the environment [8,39–43]. Moreover, urban areas not only contribute to climate change but are also affected by its impacts [44–47]. These effects, particularly heat waves, disproportionately affect vulnerable community groups such as the elderly, the infirm, and young children [48–51].

In the context of Addis Ababa, very limited studies are available. For example, with the use of climate models [52], predicted that the mean annual maximum temperature anomalies would exhibit an increase of 1.3–1.5 °C during the 2030s, 2.0–3.0 °C during the 2050s, and 4.0–5.0 °C in the 2080s. Similarly [53], conducted downscaling of future temperature and precipitation extremes in Addis Ababa. The maximum temperature increase at Addis Ababa Observatory was found to be in the range of 0.9 °C in 2020 to 2.1 °C in 2080. The minimum temperature is projected to increase by 0.3 °C in 2020 and 1.0 °C in 2080. Moreover [48], focuses on climate change and trend analysis of temperature in Addis Ababa. The analysis was based on the difference in temperature between Bole and Entoto stations. The study found that the annual temperature trend analysis for Bole station exhibits a positive trend that is statistically significant. While the Entoto station insignificantly increased.

While several temperature trend analyses have been conducted in Ethiopia [29,54–57], studies specifically focusing on Addis Ababa, the capital city, are limited. This study aims to bridge this gap by using grid data to provide a dynamic understanding of temperature trends over the past 38 years (1981–2018) within Addis Ababa. The objective is to comprehensively assess historical temperature trends, incorporate climate information into long-term urban planning, develop effective adaptation strategies, and enhance climate monitoring at the city scale. Moreover, by concentrating on temperature variability in a metropolitan area, this research contributes to the cumulative knowledge in the field of climate science concerning urban areas and provides insights essential for sustainable urban development and climate resilience planning [58].

2. Materials and methods

2.1. Description of the study area

Addis Ababa is the capital city of Ethiopia and the diplomatic center of Africa [59,60]. The 2010 Central Statistical Agency (CSA) of Ethiopia estimates the population of Addis Ababa at 3.3 million, although the UN-Habitat believes the population is closer to 4 million [61]. Geographically located at the heart of the nation, 9°2′ N latitude to 9°5′ N and 38°45′ E longitude (Fig. 1), it covers an area of about 540 km^2 [53,62,63]. Administratively, the city consisted of eleven sub-cities with an average altitude of 2400 m above mean sea level, with the highest elevation at Entoto Hill to the north reaching 3200 m [59]. Over the past 60 years, Addis Ababa has experienced an average maximum temperature of 22.9 °C and a minimum temperature of 10.2 °C [64]. Minimum and maximum temperatures increased by 0.4 °C and 0.2 °C every decade, respectively, from 1951 to 2002 [65].

The population density of Addis Ababa city varies from one sub-city to another. The highest population was registered in Addis Ketema sub-city with a population of 7215/sq.km, compared to the sparsely populated area in Akaki-Kality sub-city, which had a population of 1832p/sq.km. Despite all this, sub-cities in the downtown area are densely populated than those in the surrounding districts [63,66].

The weather and climatic conditions of Addis Ababa are largely influenced by its topography; the altitude ranges between 2100 and 3200 m above sea level [67]. Because of the geographic location, economic opportunities, capital city of the country, political and diplomatic center, and due to the political instability in regional towns, an overwhelming number of populations migrated towards the city. As a result, the population has been increasing alarmingly over the past decade. Recent studies underscore that in Ethiopian cities, the rate of urbanization outpaced population growth [68]. It is evident that, as a result of the rapid rate of population growth in the city, the areas covered by vegetation, forests, and urban agriculture have been replaced by built-ups; consequently, the proportion of vegetation has significantly dropped and dominated by industries and settlements. This could ultimately disturb the local climate and ecology. In connection with this [58,63,69], reported that in Addis Ababa city, climate change and its associated impacts were further intensified by an unprecedented rate of urbanization and population growth.

2.2. Data sources and types

The study was conducted using data acquired from the National Meteorological Agency of Ethiopia. This dataset comprised monthly time series records of maximum and minimum temperatures spanning a thirty-eight-year period from 1981 to 2018, with a spatial resolution of 4 km × 4 km. The researchers intended to use meteorological data covering a time span of 40 years. However, due to a lack of the required years (1981–2020) of data from the Ethiopian Meteorological Agency, the researchers were obliged to use only the available data from 1981 to 2018. In this study, a total of 120 grid points, including proxy stations were considered as inputs to generate the continuous interpolated raster surface. As established in the existing literature, temperature serves as a fundamental indicator of climate conditions and is frequently employed to assess the rate and magnitude of change [70,71].

In accordance with this perspective, the World Meteorological Organization (WMO) has emphasized that a 30-year timeframe serves as the reference period for climate analysis [72]. The present study aligns with the criteria outlined by the World Meteorological Organization, ensuring that it meets the standards for climate research.

The data obtained has been checked against its logical consistency, missing values, and completeness based on the suggestion by Ref. [73]. In this study, a total of 120 grid points was used as an input and analyzed the variability and trends of temperature at monthly, seasonal, annual, and decadal time scales (Fig. 2). The purpose was to reveal the anomaly and trend of change of both maximum and minimum temperature across time and space in the period of concern. As literatures underscore, the use of grid data has

gained significant attention, particularly in the field of hydro- climatology and disaster risk assessment [74].

2.3. Geostatistical models

This study explores the application of geostatistical models, which play a pivotal role in predicting values at locations not included in sample areas, all the while offering a quantification of the associated prediction uncertainty. This topic has been thoroughly examined in the studies conducted by Refs. [75–77]. To facilitate this predictive process, two primary interpolation techniques exist: deterministic and geostatistical [78]. The geostatistical method is a viable alternative to deterministic methods for spatial data interpolation [79]. The geostatistical interpolation method, among others, includes original kriging, simple kriging, and universal kinging that can obtain a good simulation result [80]. Ordinary kriging is the most widely used geostatistical interpolation method, and it is an ideal method of spatial prediction that weights the surrounding observed measured points to calculate a prediction for an unknown position [81–83]. Geostatistical methods have been rated superior to deterministic approaches [83–87]. It is increasingly preferred and more popular since it enables one to use the geospatial correlation between points to estimate the attribute location of unsampled places [75,80], and [81]. It is also one of the most accurate estimation methods, since it examines several factors, including the distance between points and spatial variability [88].

This study mainly relied on the gridded meteorological data of monthly maximum and minimum temperatures. In this regard, gridded estimates of weather parameters that integrate satellite and unevenly distributed on-ground observations are a potential alternative [89]. There is no significant difference between station data and combined gauge-satellite products; nevertheless, the combined product has higher quality and is widely used in countries like Ethiopia, where stations are sparsely located [90–92]. There are advantages to utilizing gridded products over in-situ temperature measurement when meteorological stations are limited, there is uneven station distribution, and there are a large number of missing data and data quality issues [93–96]. In comparison to gauge measurements, satellite estimations truly represent spatial heterogeneity [17]. Satellite remote sensing technology also offers distinct advantages over ground-based observation, including long-term, wide-scale, and low cost [97]. Moreover, the advantage of gridded datasets over gauge observation is that it provide a long record of time series data, can enhance data intensity due to their high spatial coverage, and permit data extraction from a number of locations [98]. For the aforementioned reasons, gridded datasets were widely used in a number of previous studies [99–102].

2.3.1. Kriging

Geostatistical methods are widely applied to interpolate with climate variables [103–107]. Ordinary, simple, co-kriging, universal, regression, and residual kriging are all types of stochastic interpolation under the kriging category [108,109]. Kriging is a more
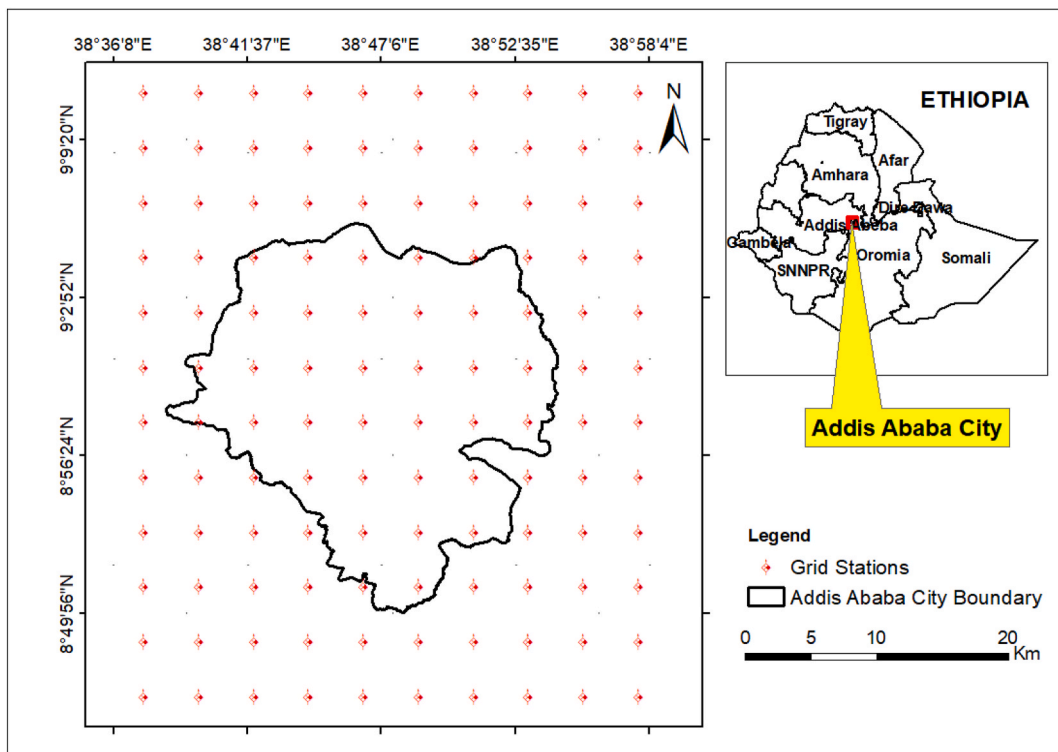

Fig. 2. Spatial distribution of grid stations.

sophisticated method than other interpolation techniques because it provides the best linear unbiased estimator for the interpolation problem [84,110]. It helps to calculate the semi-variogram, and the interpolation analysis of error is provided [84]. The kriging method will give the lowest error, followed by the inverse distance square and the inverse distance method [111].

In this study, geospatial technologies, namely geostatistical analysis methods, were used to evaluate time series gridded metrological data of minimum and maximum temperature using the kriging approach [112]. This is due to the fact that kriging produces better estimates than other techniques [113]. It is therefore widely used for spatial interpolation, with the main advantage of including the spatial correlation of data [114]. Ordinary kriging outperforms the other methods [79,100,106], and [107]. Ordinary kriging is frequently applied in meteorology studies [109,115].

Hence, in this study, ordinary kriging was employed in order to analyze time-series climate variable data. This is because the target variable was temperature, which has spatial variance characteristics [116]. The equation (Eq. 1) used in ordinary kriging is as suggested by Refs. [117,118].

$$\widehat{Z}(s_o) = \sum_{i=1}^{N} \lambda_i Z(s_i) \tag{1}$$

where;

$Z(s_i)$: the measured value at the i th location

λ_i: an unknown weight for the measured value at the i th location

(s_o): the estimation location

N: the number of measured values

With kriging method, the value $\widehat{Z}(s_o)$ at the point S_0, where the true unknown value is $\widehat{Z}(s_o)$, is estimated by a linear combination of the values at N surrounding data points [119].

2.3.2. Temperature trend analysis

The examination of temperature trends is a crucial aspect of climate analysis. One essential statistical measure employed in this analysis is the coefficient of variation (CV). CV serves as a valuable tool for assessing the year-to-year variability within temperature datasets, presenting the degree of variation as a percentage relative to the mean temperature [25,120]. The CV (Eq. (2)) was computed using the following equation [121–125]:

$$CV = \left(\frac{\sigma}{\mu}\right) * 100 \tag{2}$$

here, CV represents the coefficient of variation, where σ denotes the standard deviation, and μ signifies the mean temperature record. By employing this formula, the overall variability was effectively quantified within the temperature records of a specific region. Accordingly, the CV values of temperature variability are categorized as low (CV<20%), moderate ($20 < CV < 30$), high ($CV > 30$), very high ($CV > 40$) and extreme ($CV > 70$) [102,125,126]. These categories aid in interpreting the extent of temperature fluctuations within the dataset reflecting that a larger CV indicates a higher variance in climate variables, while a smaller CV implies more stability [95]. Consequently, the analysis focuses on assessing the spatial variability of minimum and maximum temperatures for the study period. It is organized into seasonal perspectives (Kiremt, Belg, and Bega) and an annual overview. This comprehensive approach enables us to gain valuable insights into temperature trends and their potential implications for the area under investigation.

2.3.3. Standardized anomaly index (SAI)

In this study, the number of cooling (-ve) and warming (+ve) years, as well as the frequency and severity of dry and wet years, were all determined using the standardized anomalies index [120,122,124]. The standardized anomaly index (Eq. (3)) can be calculated using the following equation:

$$SAI = \frac{(X - \overline{X})}{\sigma} \tag{3}$$

here, SAI represents the standardized anomaly index, where × denotes the yearly and seasonal mean temperature for a specific year, $\overline{X}$ signifies the mean annual and seasonal temperature across the observation period, and σ represents the standard deviation of the annual and seasonal temperatures observed throughout the study period.

Based on SAI, the intensity of the drought is categorized as follows: no drought ($SAI > -0.84$), moderate drought ($-0.84 > SAI > -1.28$), severe drought ($-1.28 > SAI > -1.65$), and extreme drought ($SAI < -1.65$) [127]. This standardized anomaly index, along with its associated drought severity classifications, forms a critical component of the study's methodology for assessing temperature variations and their implications on climate trends.

2.3.4. Modified Mann-Kendall test

As the literature suggested, there are two fundamental tests commonly used in the field of climate science to determine the significance level of time series metrological data: parametric and non-parametric techniques [128,129]. The parametric test requires a normal distribution of datasets. However, the non-parametric test is a distribution-free technique and requires only independent time series datasets [130,131]. Nonparametric methods are commonly used in trend analysis due to their ease of calculation and relatively low number of assumptions [132]. Among the various statistical methods, the Modified Mann-Kendall (MMK) test is the most widely

used as it determines the nature of the trend along with its significance [133]. Because of the advantage of handling serially correlated datasets, MMK is preferred over MK [134,135]. In this study, the Modified Mann–Kendall test and Sen's Slope estimator tests were used to assess the monthly, annual, and seasonal (*Kiremt*, *Belg* and *Bega*) temperature trend for the period of 1981–2018 using R programming.

Literature underlines that the Modified Mann-Kendall (MMK) test is largely used to detect whether there is a decreasing or increasing trend in time series of climate data [122,136–139]. Sen's slope estimator and the modified Mann-Kendall are the two prominent non-parametric techniques for trend analysis of hydroclimatic data. The monotonicity of time series data and statistical significance are provided by MMK trend [140].

According to Refs. [141–144] the Kendall's test statistics S is computed using the following formula (Eq. 4 and 5):

$$S = \sum_{i=1}^{n-1} \sum_{j=i+1}^{n} Sgn(X_j - X_i) \tag{4}$$

$$Sgn(X_j - X_i) = \begin{cases} +1, if(X_j - X_i) > 0 \\ 0, if(X_j - X_i) = 0 \\ -1 \quad if(X_j - X_i) < 0 \end{cases} \tag{5}$$

For a time series x_i that is ranked from $i = 1, 2, ...n$-1; and xj, which is ranked from $j = i + 1, i + 2, ...,n$, where n is the total number sample points [145]. For $n > 10$, S follows approximately normal distribution with a mean zero and variance given by Eq. 6

$$E(S) = 0$$

$$Var(S) = \frac{n(n - 1)(2n + 5) - \sum_{i=1}^{m} t_i(t_i - 1)(2t_i + 5)}{18} \tag{6}$$

where t_i considered the number of ties up to the sample i. The original Mann-kendall test, which computes (Eq. (6)) variance, makes the assumption that autocorrelation between data points is negligible, which is not always the case [146]. For this reason [133], recommended a Modified Mann-Kendall test that takes into account the autocorrelation structures for all lags in a sample by multiplying the variance by a correlation factor. The same source further explained that the modified variance V*(S) is given as [147] Eq. 7

$$V^*(S) = VAR(S) \bullet C_f \tag{7}$$

where C_f represents a correlation factor by the empirical expression (Eq. (8)):

$$C_f = 1 + \frac{2}{n(n - 1)(n - 2)} * \sum_{i=1}^{n-1}(n - i)(n - i - 1)(n - i - 2)\rho_i(i) \tag{8}$$

where $\rho_s(i)$ the serial autocorrelation in the data series.

The MMK test statistic in Z denoted by Eq. (9) [148].

$$Z_{MMK} = \begin{cases} S - 1 \Big/ \sqrt{V^*}(S), if \ S > 0 \\ 0 \quad if \quad S = 0 \\ S + 1 \Big/ \sqrt{V^*}(S) \ if \ S < 0 \end{cases} \tag{9}$$

where Z_{MMK} follows a standard normal distribution. A positive Z value means an upward trend and vice versa. A significant level also utilized to denote either an upward or downward trend in a two-tailed test [147]. The trend to be significant, the value of Z should be > 1.96 or < -1.96 corresponding to the significant level of 0.05 [149].

2.3.5. Sen's slope estimator

Sen's slope estimator was used to evaluate the MMK test's relative strength in the processing of time series meteorological data [150]. In comparison to the linear regression approach, it minimizes the influence of no data value or outliers on the slope [122, 151–153]. Sen's slope estimations are frequently employed to ascertain the strength of trends in long-term temporal data [154,155]. The rate of the increasing/decreasing trend in climate data was calculated using the non-parametric Sen's slope estimator by applying the equation below [150,156].

The trend is calculated as expressed in Eq. (10):

$$\beta = Median\left(\frac{X_j - X_i}{j - i}\right), j > i \tag{10}$$

where β is Sen's estimate. A time series rising trend is indicated by β > 0. Otherwise the data set shows a declining tendency during the course of the investigation. The method is more reliable than linear regression, in that it lowers the effect of outliers and no data values and performs better even with regularly distributed data [157]. In this study, Sen's slope is used to determine the trend's magnitude of maximum and minimum temperatures. Since temperature data was not normally distributed as a result the Mann-Kendall and Sen's

slope estimator was preferred and utilized to detect the trends and slopes respectively [158].

2.3.6. Principal component analysis (PCA)

Principal component analysis is a method that reduces a dataset's dimensionality significantly, making it easier to analyze while reducing information loss [159,160]. Principal component analysis (PCA) is a multivariate statistical method used to investigate correlations between several variables and uncover their fundamental structures [161]. The theory and application of PCA are used to analyze the influence of particulate variables on climate change [162] through climate pattern analysis [163,164]. The PCA enables the identification of components and reduction of the number of factors influencing the particle concentration [162]. PCA identifies two or more elements that are necessary to explain each variables influence and contribution [165]. Principal component analysis is a versatile tool utilized in meteorological studies. It has been applied extensively to comprehend, analyze, and reconstruct large multivariate climate datasets [166–168]. PCA extracts eigenvectors and eigenvalues from the original variables of the covariance matrix. The eigenvectors are multiplied by the original corrected variables to obtain the list of principal components [169].

The objective of PCA is to reduce the number of variables; it is essentially intended that each variable co-varies with the other variables as little as feasible [165,170]. The variance in PCA analysis is computed with respect to each and every variable (monthly, annually, and seasonal). The variables considered in this study were temperature (maximum, minimum, and average temperature). The only variables taken into account in each principal component analysis were those with the highest correlation coefficients (absolute values) [162,166]. In this study, PCA was performed mainly in order to show the influence and relevance of temperature variables in a climate change scenario. The analysis was performed for the period 1981–2018 on a monthly, annual, and seasonal basis.

Each variable was represented by a vector on the plot, which showed how all variables depended on the principal components. The strength and dependency of a particular component are shown by the vector's length and direction. The vector's placement within a certain quadrant of the coordinate system signifies whether these factors have a positive or negative effect on a particular component. Closely spaced vectors on the graph indicate that all of the variables represent the same variation in the system, therefore using any one of them will be sufficient for additional analysis. A positive correlation is indicated by an acute angle formed by vectors of the various variables; a negative association is represented by an obtuse angle, and no relationship is denoted by a right angle [162].

There are a number of statistical programs available that include the implementation of principal component analysis (PCA). The two well-known "R" functions, princomp and prcomp, construct PCA by utilizing standard deviation and eigen decomposition, respectively. In this study, *prcomp* command of R statistical software is used [166,167].

Biplots.

The biplots were informative, and interpretations were summarized as follows [170–172].

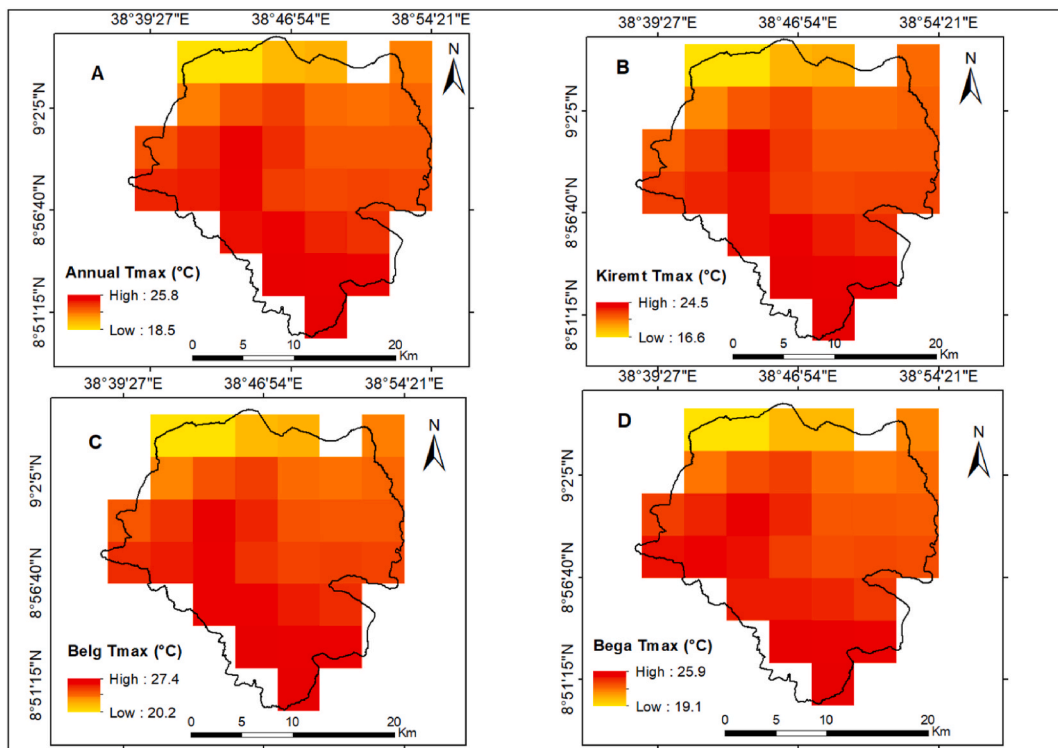1. In the scatter plots, closer points correspond to observations of similar scores in PCs.

Fig. 3. Mean annual and seasonal maximum temperature: Annual (A), *Kiremt* (B), *Belg* (C) and *Bega* (D) of Addis Ababa (1981–2018).

2. A set of elements having a similar origin is made up of elements that are mutually associated.
3. The length of a vector provides information about the variance.

The greatest amount of variation for the entire datasets is represented by the first component (PCA1), whereas the maximum variance that remains in the residual datasets is accounted for by the subsequent components [173].

3. Result and discussion

3.1. Variability of maximum and minimum temperature in annual and seasonal basis

The mean annual, seasonal maximum, and minimum temperatures in Addis Ababa varied both spatially and temporally. As Figs. 3A and 4A show, the average annual maximum and minimum temperatures were 25.8 °C and 12.6 °C, respectively. As compared to other seasons, the highest maximum and minimum temperatures were 27.4 °C and 13.8 °C, respectively, recorded during the spring (*Belg*) season (Figs. 3C and 4C). Winter (*Bega*) season average maximum and minimum temperatures found to be 25.9 °C and 11.4 °C, correspondingly (Figs. 3D and 4D). The main rainy (*Kiremt*) season average maximum temperature was 24.5 °C (Fig. 3B) and the minimum temperature was 13.3 °C (Fig. 4B).

The spatial distribution of seasonal average maximum and minimum temperatures (Figs. 3 and 4) revealed that the southern part of Addis Ababa was the hottest, where the maximum temperature was recorded. While the northern part of the city was the coolest, where the minimum temperature was observed. This is because the northern edge of the city is covered by dense forest, while the hottest southern is found in relatively lower elevation. From this, it is possible to deduce that temperature and elevation have a direct relationship. It is a universal truth that for every 167 m altitude, there is a decrease in temperature of 1 °C. In connection with this, the proximity of Ethiopia to the equator as well as the intricacy nature of the country's topography have a significant influence Ethiopia's climate, particularly the temperature [174,175]. Similarly, physical features such as terrain and sub-basin characteristics typically influence the spatial variability of maximum and minimum temperatures [120].

Among the different seasons, comparatively, *Belg* was found to be the hottest. This is because *Belg* season includes months of March, April, and May which are the hottest months of the year. Usually it is during these months that the maximum temperature is noticed [176]. Likewise [177], summarized the earlier research done in several regions of Ethiopia and found that there was regional and temporal variability in temperature.
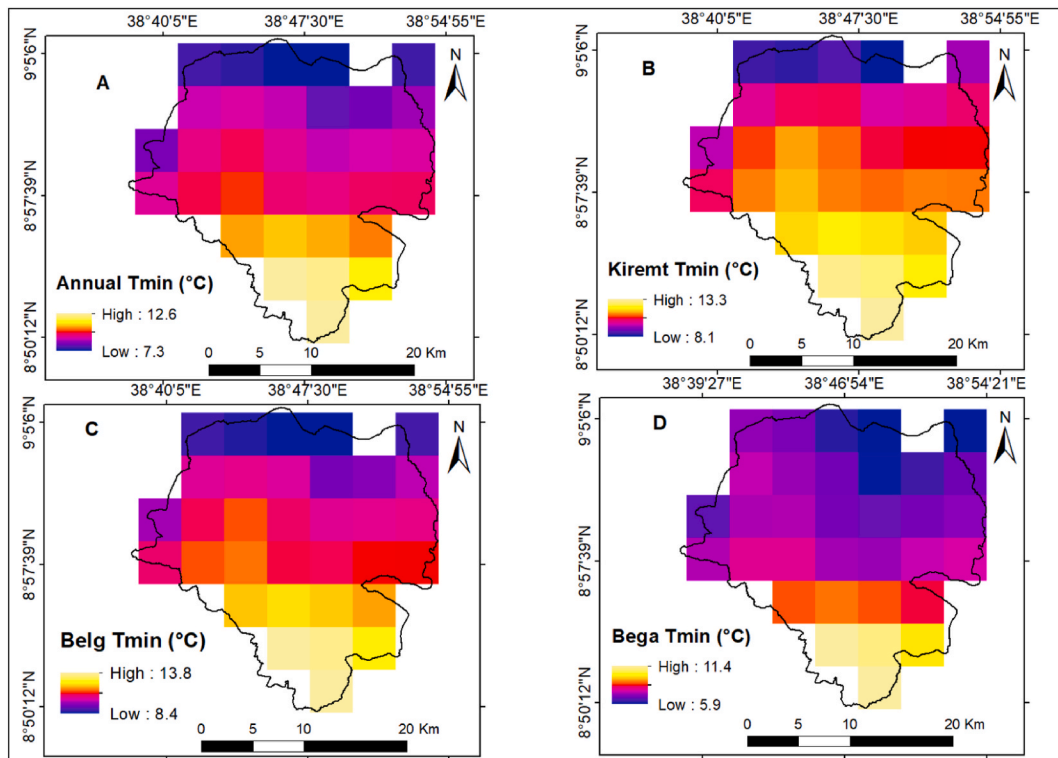

Fig. 4. Mean annual and seasonal minimum temperature: Annual (A), *Kiremt* (B), *Belg* (C) and *Bega* (D) of Addis Ababa (1981–2018).

3.2. Coefficient of variation in annual, seasonal maximum, and minimum temperature

Across the study period, the annual and seasonal average maximum temperature coefficients of variation were less variable as CV<10% (Fig. 5A–D). Likewise, the mean annual and seasonal minimum temperature have shown low variability (Fig. 6A–D). In both cases of the maximum and minimum temperatures coefficients of variation, low variability of temperature was observed during the *Belg* season, where the calculated CV ranges between 2 and 4%. Generally, the average minimum temperature showed a relatively higher degree of variability as compared with the maximum temperature in both annual and seasonal time scales, as observed in Figs. 5 and 6.

3.3. Variability of monthly maximum and minimum temperature

The spatial distribution of the average monthly maximum and minimum temperature for the observation period (1981–2018) is shown in Figs. 7–9. It was in August that the monthly average maximum temperature dropped to its lowest value of 23.37 °C (Figs. 7 and 8). In the of March, the average maximum temperature reached its peak of 27.59 °C (Fig. 8). Following that, both the high and low temperatures gradually declined. The highest monthly minimum temperature was recorded in May, 14.33 °C, whereas the lowest temperature was registered in December (10.70 °C) (Figs. 7 and 9).

The highest average monthly maximum temperature was recorded in the months of March (27.59 °C), April (27.03 °C), and May (27.52 °C). Similarly, it was in the months of March (13.12 °C), April (14.01 °C) and May (14.33 °C) that the highest minimum temperature was detected. During the months of March and December, the study area experienced the highest monthly average maximum and lowest minimum temperature, with the values of 27.59 °C and 10.7 °C, respectively. The average maximum temperature fell to its lowest point in the main rainy (*Kiremt*) season, the months of July (23.79 °C), August (23.37 °C), and September (24.65 °C). Similarly, the lowest minimum temperature was registered in the autumn season (October, November, and December).

Figs. 10 and 11 show the average monthly maximum and minimum temperature coefficients of variation analysis results between 1981 and 2018. Overall, the monthly maximum temperature analysis result exhibited a normal variance of CV < 20%, throughout the twelve months. On the other hand, the average monthly minimum temperature demonstrated a minimal variance with a CV<20% from March to September. In October and February, there was a moderate variance (CV<30%). It is possible to deduce that the minimum temperature was relatively more variable as compared with the maximum temperature. During the months of November (CV = 30.78%), December (CV = 35.47%), and January (CV = 30.23%), the minimum temperature coefficients of variations were relatively higher.
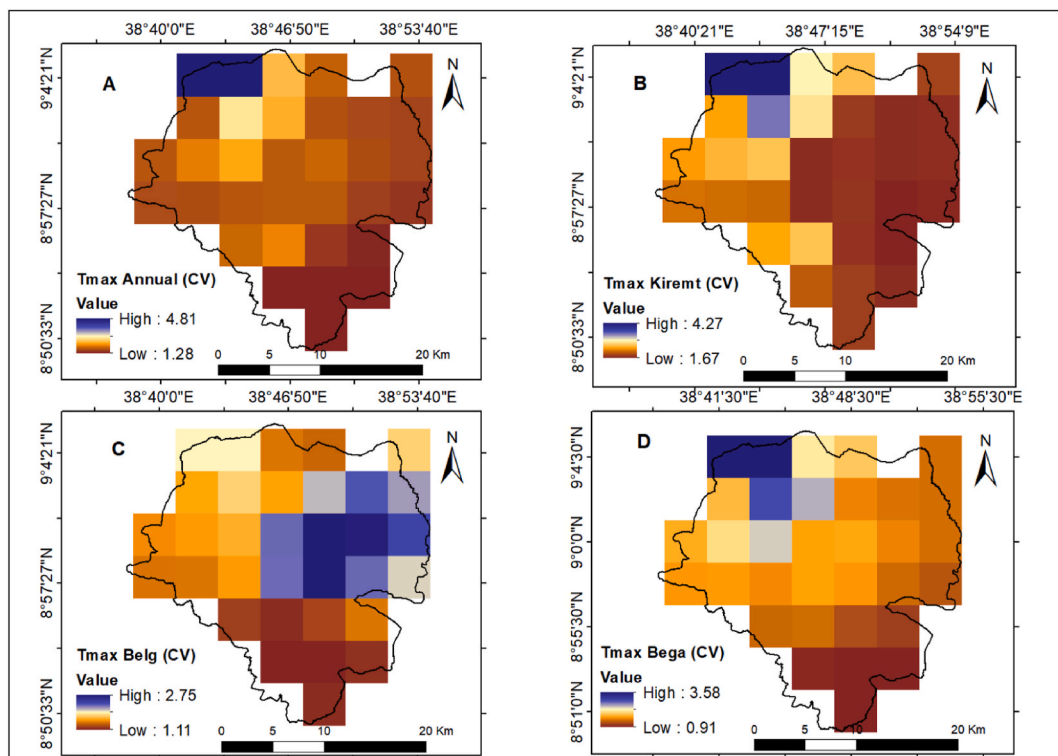

Fig. 5. Cofficient of variation of maximum temperature: annual (A), *Kiremt* (B), *Belg* (C), and *Bega* (D) over the study period (1981–2018).
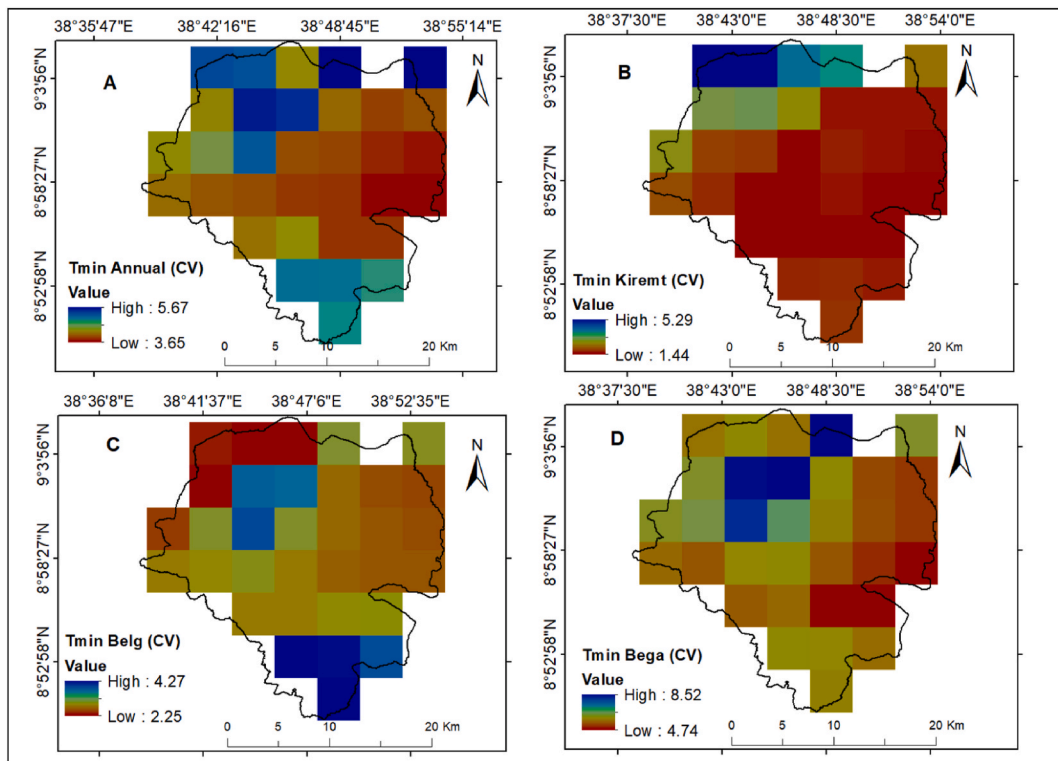
Fig. 6. Cofficient of variation of minimum temperature: annual (A), *Kiremt* (B), *Belg* (C), and *Bega* (D) in the period of concern (1981–2018).
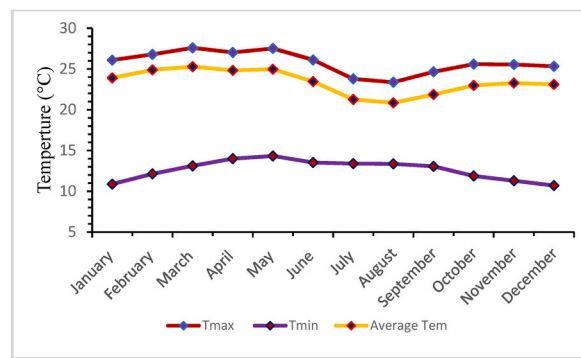

Fig. 7. Monthly average temperatures of maximum, minimum, and average for the period from 1981 to 2018.

3.4. Standardized anomaly index of maximum and minimum temperature

Throughout the observation period (1981–2018), the standardized temperature anomalies (STA) of mean annual and seasonal maximum temperatures followed a similar pattern. The analysis result of the maximum temperature stipulated that, over the last two decades (1998–2018), the warming effect (positive anomaly) was sharply intensified across all seasons (Fig. 12A–C, and D) except in Kiremt season (Fig. 12B), where the maximum temperature anomaly was relatively less pronounced. While the warming effect is evident in all the other seasons, the increment of maximum temperature anomalies varies among seasons. In connection to this, the study also draws a comparison to previous research in the northern region of Ethiopia, which found a gradual increase in average maximum temperatures between 1983 and 2016. This highlights the long-term nature of the warming trend, spanning several decades [178]. Rising temperatures have the potential to have significant effects on a number of facets the environment and society.

The analysis findings shown in Fig. 13, where the minimum temperature over the last 38 years illustrates how Addis Ababa city consistently experienced both warming and cooling years (Fig. 13A–D). The SAI of annual and seasonal minimum temperatures accounts for 65% of warming years and 35% cooling years. The graph (Fig. 13A–D) illustrated that the standardized anomaly index betweeen 1981 and 1996 showed a negative anomaly across the four seasons (annual, *Kiremt*, *Belg* and *Bega*). From 1997 to 2009, a
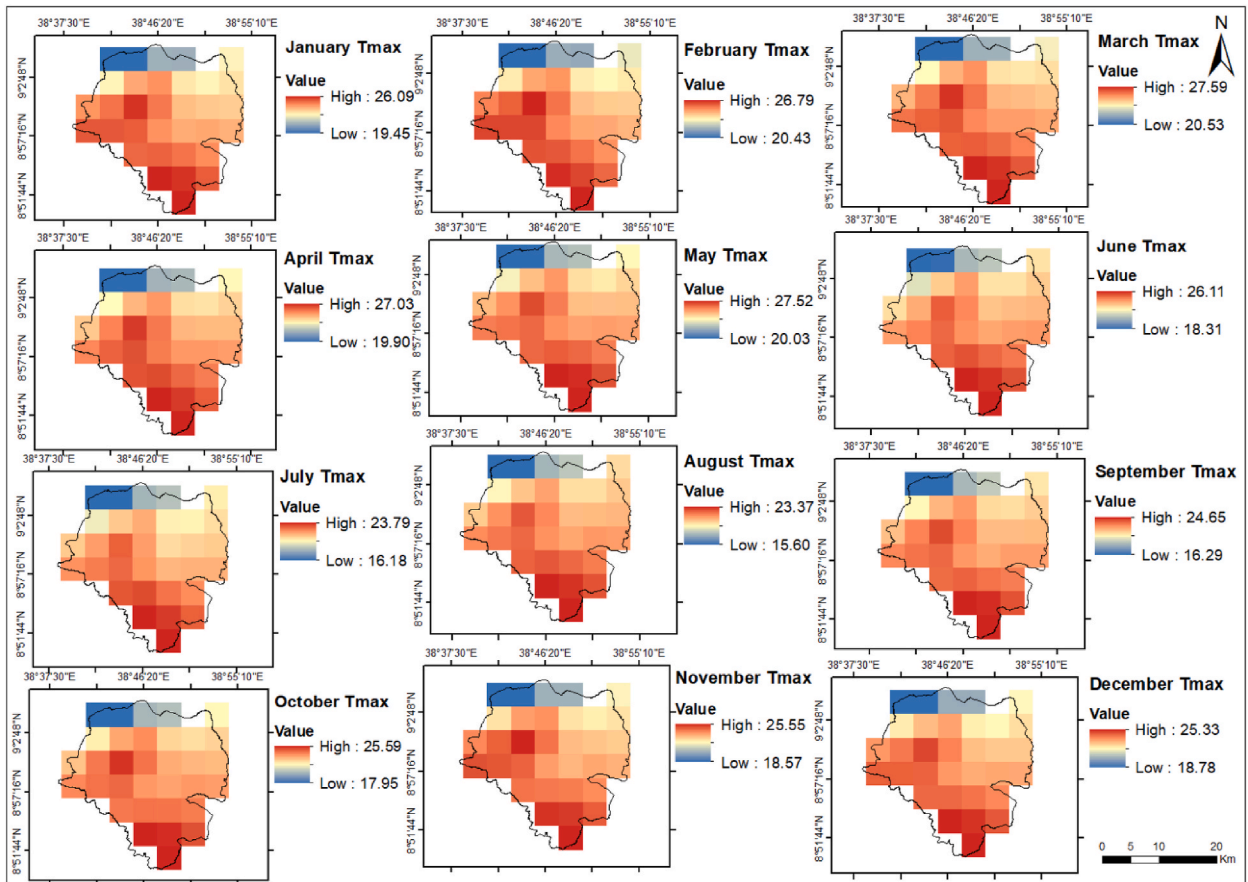
Fig. 8. Spatial distribution of average monthly (January to December) maximum temperature of Addis Ababa (1981–2018).

positive anomaly was observed in both annual and seasonal minimum temperatures. However, from 2010 on, a negative anomaly completely dominated the observations. The number of years with negative anomalies was greater than the number of years with positive anomalies. This indicates that Addis Ababa has experienced more dry years than wet years. The findings of the study also designated the 1980s and 2010s as dry years as compared with the 1990s and 2000s, which were wet years.

3.5. Temperature trend analysis

The result obtained from the trend analysis (Fig. 14) revealed that there was a positive trend in the average annual, seasonal maximum, and minimum temperatures across the observation period (1981–2018). Studies conducted in southern Ethiopia indicated a significant warming trend of seasonal and annual mean temperatures between 1980 and 2015 [179]. The result of the maximum temperature was statistically highly significant, as the calculated p-value was 0.0001, which is lower than the threshold significant level (P < 0.05) (Fig. 14A–D). The same is true for the average annual and seasonal (*Kiremt*, *Belg*, and *Bega*) minimum temperatures in which the calculated P value was slightly lower than the maximum temperature (Fig. 14E–H).

The long-term average maximum temperature for the annual, *Kiremt*, *Belg*, and *Bega* seasons were 25.8 °C, 24.5 °C, 27.4 °C, and 25.9 °C, respectively. On the other hand, the average minimum temperature for annual (12.6 °C), *Kiremt* (13.3 °C), *Belg* (13.8 °C), and *Bega* (11.4 °C). The highest temperature for both the maximum (27.4 °C) and minimum (13.8 °C) temperature was registered during the spring (*Belg*) season. The catter plot showed that the rate of increase of the average annual and seasonal maximum temperatures was far higher than the minimum temperature (Fig. 14A–D). In contrast, the average annual and seasonal minimum temperature increment was a moderate one (Fig. 14E–H). The linear regression analysis also found that fluctuations in maximum temperature tend to vary with a coefficient of determination (R^2) ranging from 0.66 spring (*Belg*) to 0.80 annual.

With regard to the maximum temperature, the highest average annual minimum and maximum temperatures were registered in 1985 and 2016, with the values of 24.23 °C and 29.35 °C, successively. The highest average annual maximum temperature for *Kiremt* and *Belg* seasons were 28.23 °C and 32.93 °C, correspondingly, both recorded in the same year, 2016. The yearly seasonal average maximum temperature for *Bega* season was 29.62 °C, registered in 2015 (Table 1). On the other hand, the minimum average annual, *Kiremt*, and *Bega* seasons temperature were 16.79 °C, 16.86 °C, and 18.28 °C, consecutively. All of them occurred in the same year, 2007. While, the minimum temperature's lowest average value for annual was 10.09 °C, *Kiremt* 10.33 °C, and *Bega*, 8.77 °C, it was
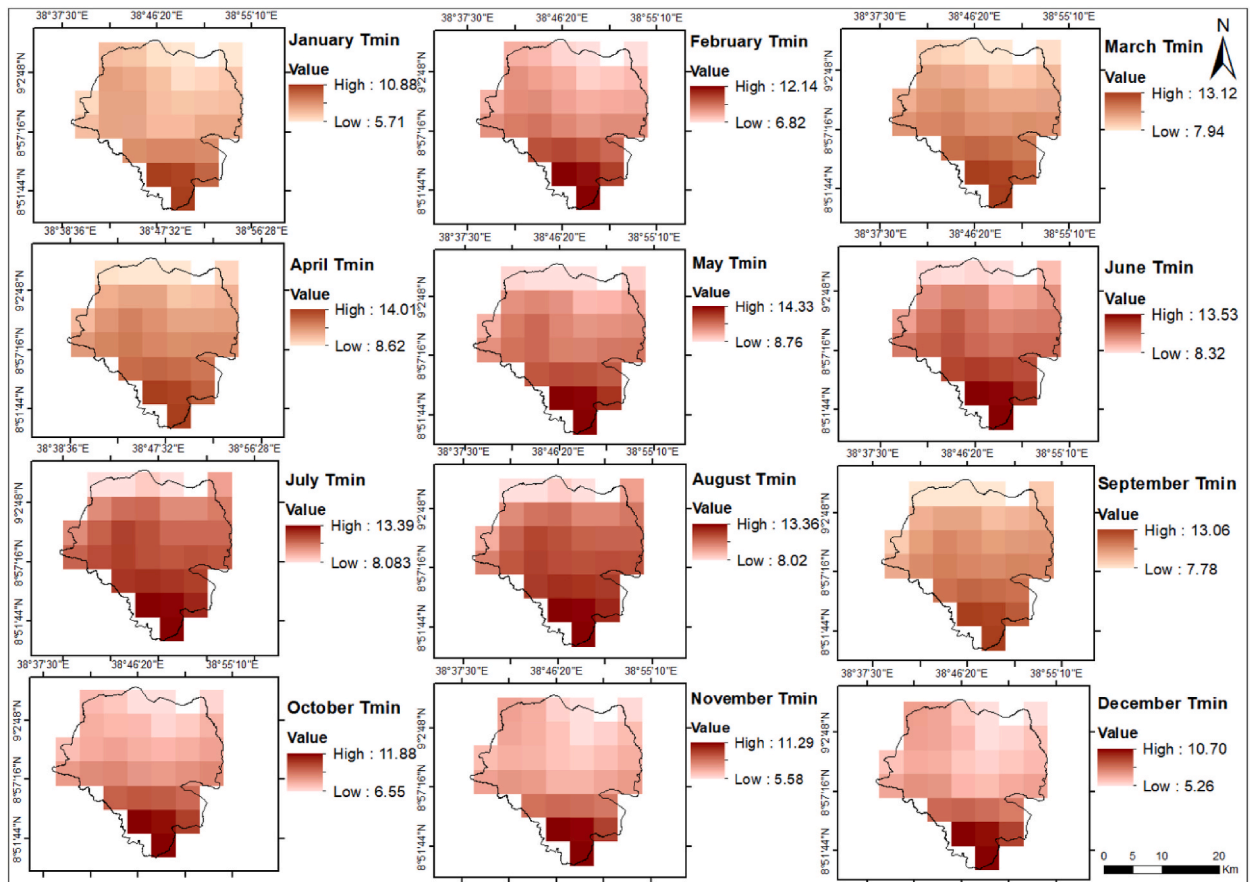
Fig. 9. Spatial distribution of monthly (January to December) average minimum temperature Addis Ababa (1981–2018).

registered in 1986 (Table 1).

Concerning the change in average annual maximum temperature across seasons, the highest temperature change occurred during the *Belg* season (Table 1). In this regard, previous studies reported that the *Belg* season, which includes the months of March, April, and May, are the warmest months where the maximum temperature is recorded during this season [120].

It is possible to understand that there was a progressive increasing trend of the average annual and seasonal maximum and minimum temperatures across the investigation period (Table 1). The results of this study, in agreement with the previous studies, reported an increasing trend in Ethiopia's annual average, maximum, and minimum temperatures [95,179]. Additionally [44], suggests that the global surface temperature is predicted to increase from 0.3 °C to 4.8 °C by the end of the 21st century. Consequently, the increasing temperature in cities like Addis Ababa could result in significant water loss, which has an impact on municipal services and domestic water supplies [180].

3.6. Decdal temperature trend analysis

Table 2 shows the average decadal maximum, minimum, and average temperatures of Addis Ababa in the period between 1981 and 2018. Based on the investigation results, it was determined that the mean annual maximum temperatures between 1981 and 1990 and 1991 and 2000 were, respectively, 24.53 °C and 25.33 °C. The standard deviations were 0.38 and 0.31, and the coefficient of variation was 1.63 and 1.31 (Table 2 and Fig. 15A and B). The mean annual maximum temperature for the third decade (2001–2010) and the last eight observation years (2011–2018) were 26.71 °C and 27.23 °C with standard deviations of ±0.73 and ±1.32 and coefficients of variation of 2.92 and 7.38, respectively (Fig. 15C and D). The analysis shows that the average maximum temperature increased by 0.8 °C during the first two decades (1981–2000). The difference in temperature between the second (1991–2000) and third (2001–2010) observation periods further escalated by 1.38 °C. The decadal maximum temperature increment over the last eighteen years (2001–2018) was soared by 0.52 °C (Fig. 15C and D). Overall, in the study period (1981–2018) the decadal maximum temperature was augmented by 2.7 °C (Fig. 15 and Table 2). In this regard, previous studies noted that the maximum temperature in the dominant parts of East Africa increased from the 1980s to the 1990s and 2000s, with Ethiopia experiencing the most changes (anomalies up to +0.9 °C) [29].

This clearly demonstrated how the temperature in the study area increases over time. On top of that, as shown in the scatter plot in
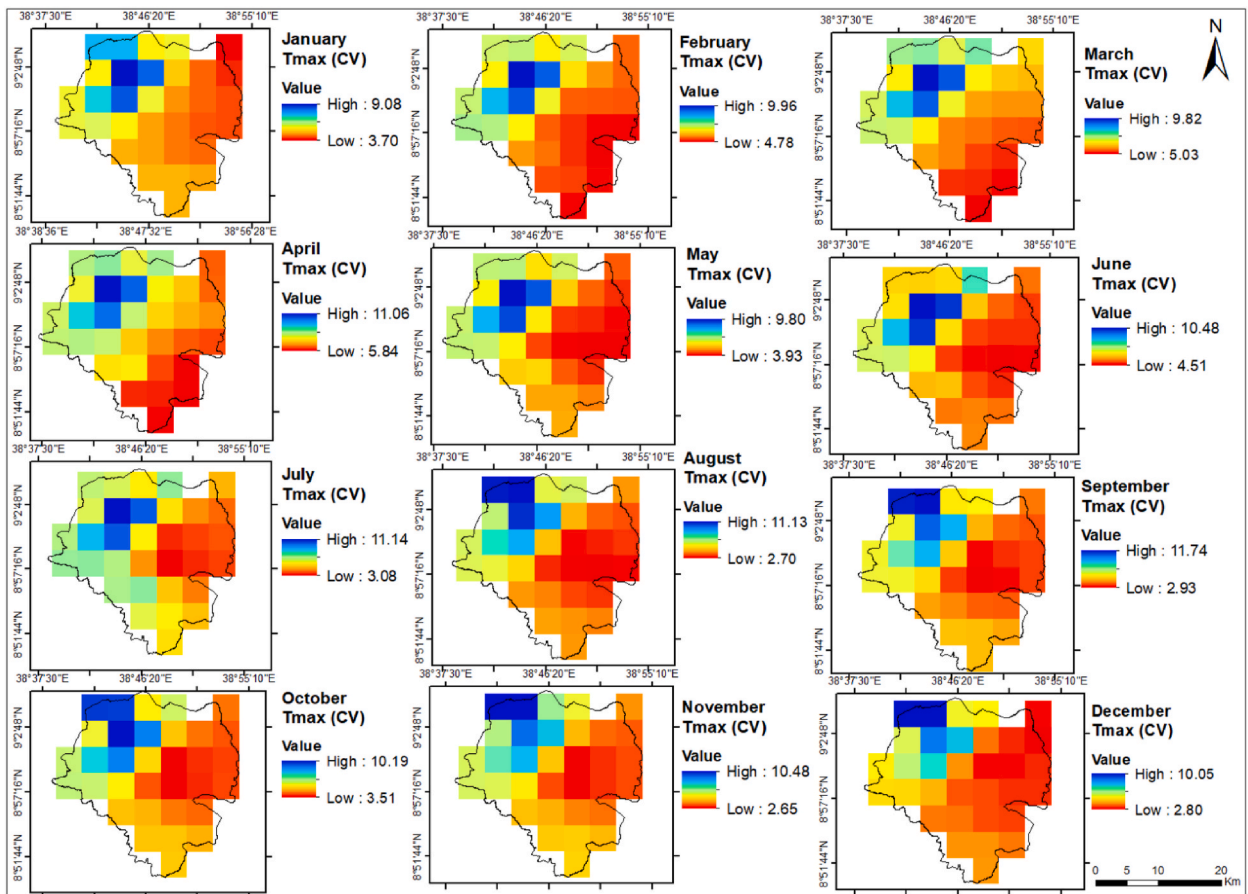
Fig. 10. Spatial distribution of monthly (January to December) maximum temperature coefficient of variation (CV) of Addis Ababa (1981–2018).

Fig. 14, the area has undergone a significant increase in mean annual maximum temperature during the last 38 years. In connection with this [53], underlines that many parts of Ethiopia have seen high temperatures during the past few decades. Previous research suggested that Addis Ababa's future maximum temperature will rise by 1–2 °C for the entire city and neighboring areas, with the greatest change occurring along the Bole, Yeka, and Akaki sub-cities in the city's east and south [58]. In this regard, the findings of this study are aligned with the reports of earlier research.

Similarly, the decadal minimum temperature difference in the first two decades (1981–2000) climbed by 1.27° (Table 2 and Fig. 16A and B). Between the second (1991–2000) and third observation (2001–2010) the temperature increased by 2.55 °C (Fig. 16B and C). In contrast, it abruptly dropped by 3.99 °C during the most recent observation period (2011–2018) (Fig. 16D). Over the study period, it is possible to understand that there was no significant increase in the decadal minimum temperature. Nevertheless, the decadal maximum temperature significantly increased across the period of observation. The mean decadal maximum and minimum temperature range between 22.48 °C and 24.36 °C, and 8.91 °C and 10.63 °C, respectively. The long-term average decadal maximum and minimum temperature increased by 1.88 °C and 1.72 °C consecutively, as stipulated in Table 2.

In the first two decades (1981–2000), the average decadal maximum and minimum temperatures scaled up by 0.45 °C and 0.64 °C, respectively (Table 2 and Figs. 15A, B and 16A, B). In the second and third observations, the average decadal maximum temperature rose by 1.05 °C. While the average decadal minimum temperature surged by 1.08 °C. By comparison, in this observation period, the temperature difference was much higher than the preceding decade. Between the third and fourth observations, the decadal average maximum temperature escalated by 0.38 °C while the decadal average minimum temperature declined by 0.22 °C. Generally, it is possible to conclude that the average decadal maximum and minimum temperatures progressively escalated through the research period, except for a slight reduction in the average decadal minimum temperature in the last observation.

3.7. Modified Mann-Kendall and Sen's slope estimator test result

3.7.1. Long-term monotonic trends of maximum and minimum temperature

Temperature trend analysis for Addis Ababa was performed using 38 years of temperature data (1981–2018). The MMK test and Sen's slope estimator statistical analysis were used to estimate the magnitude of the temperature change. The MMK test result
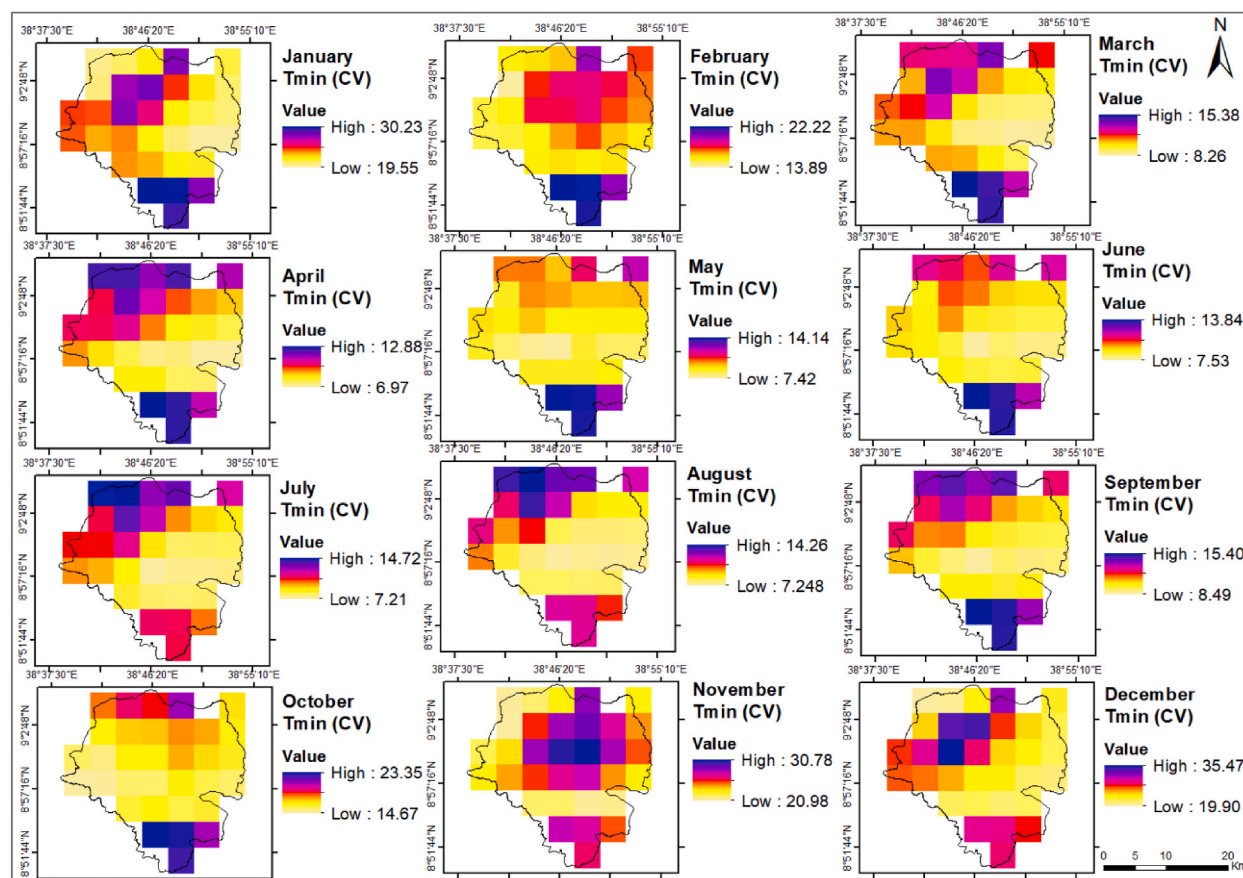
Fig. 11. Spatial distribution of monthly (January to December) minimum temperature coefficient of variation (CV) of Addis Ababa (1981–2018).

stipulated that, the Z value for maximum annual and seasonal (*Kiremt, Belg, Bega*) temperatures was 11.97, 9.70, 5.76, and 10.95, respectively as shown in (Table 3). The result of the Sen's slope estimator positive value indicated an increasing trend of maximum temperature was statistically significant as the p-value for all the seasons was less than <0.05.

Conversely, for the mean annual and seasonal minimum temperature for *Kiremt, Belg,* and *Bega,* the Z values were found to be 2.77, 2.95, 2.81 and 2.48, correspondingly. Similarly, the P values for all the seasons were less than the significant value of 0.05, which means the minimum temperature increment was statistically significant. The positive Kendall's tau value (Table 3) elucidated an upward trend for both annual and seasonal maximum and minimum temperatures. This suggests that over the study period (1981–2018), an increasing pattern in both the maximum and minimum temperatures was observed. The findings of this research aligned with the earlier studies conducted in Addis Ababa, which reported that there was a propensity for temperature increases in the study area [48]. In addition, another study conducted in South Gonder Zone underlined that there was a rising tendency in the maximum temperature [181].

3.7.2. Observed monthly maximum and minimum temperature

The results of the Modified Mann-Kendall (MKK) test and Sen's slope estimator are shown in Table 4 for both the monthly maximum and minimum temperatures of Addis Ababa between 1981 and 2018. The monthly maximum temperature has been considerably increasing throughout all months, with a P-value of 0.0001 at a significant level (Table 4). The highest monthly maximum temperatures were recorded in the months of March (27.59 °C), April (27.03 °C), and May (27.52 °C). Similarly, the greatest monthly minimum temperatures were 14.01 °C and 14.33 °C, respectively, recorded in April and May. With the exception of January and September, the increment in minimum temperature was also significant in all the months where the calculated P-value was less than 0.05 (Table 4).

3.8. Principal component analysis (PCA)

3.8.1. Annual and seasonal PCA analysis

In this section, time series maximum and minimum temperatures were analyzed at monthly, annual, and seasonal (*Kiremt*, Spring, and *Bega*) levels for the period from 1981 to 2018. As suggested by Ref. [165], PCA analysis is used in order to assess the change in

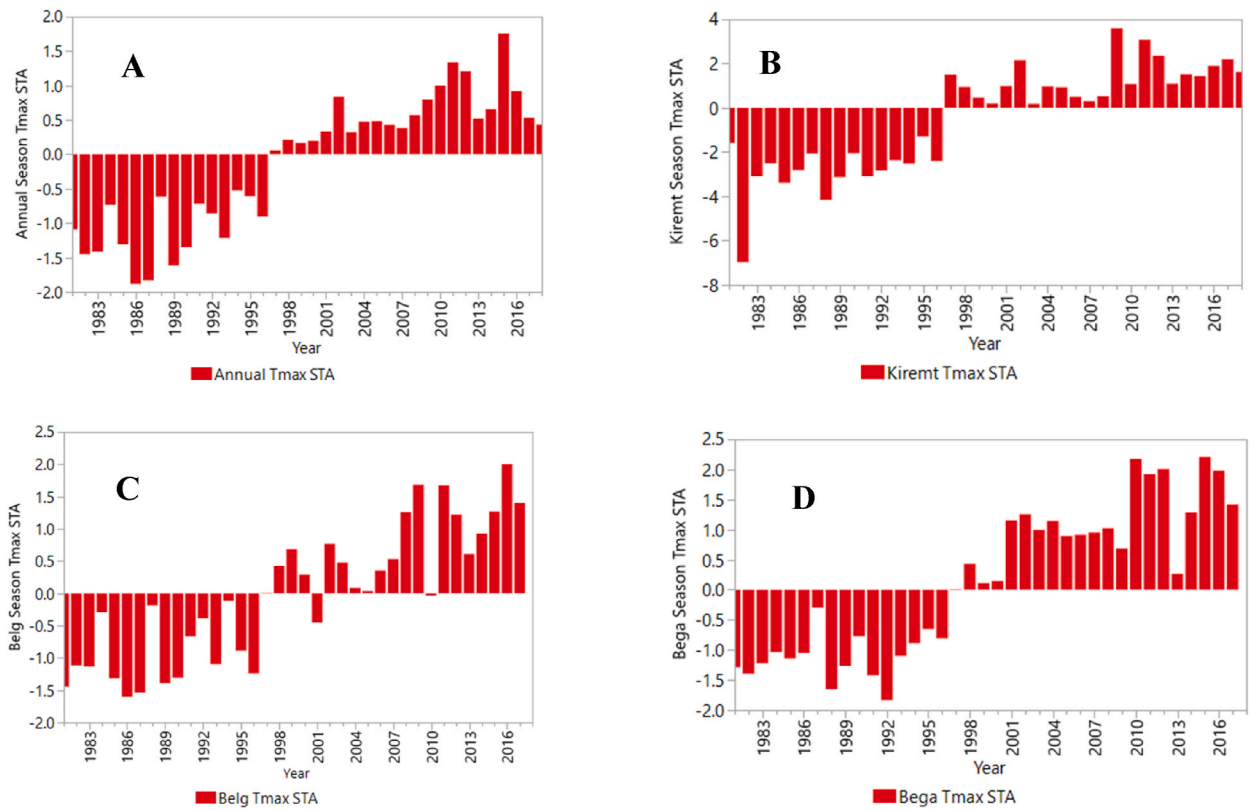**Fig. 12.** Maximum temperature anomalies for Annual (A), *Kiremt* (B), *Belg* (C), and *Bega* (D) of Addis Ababa (1981–2018).
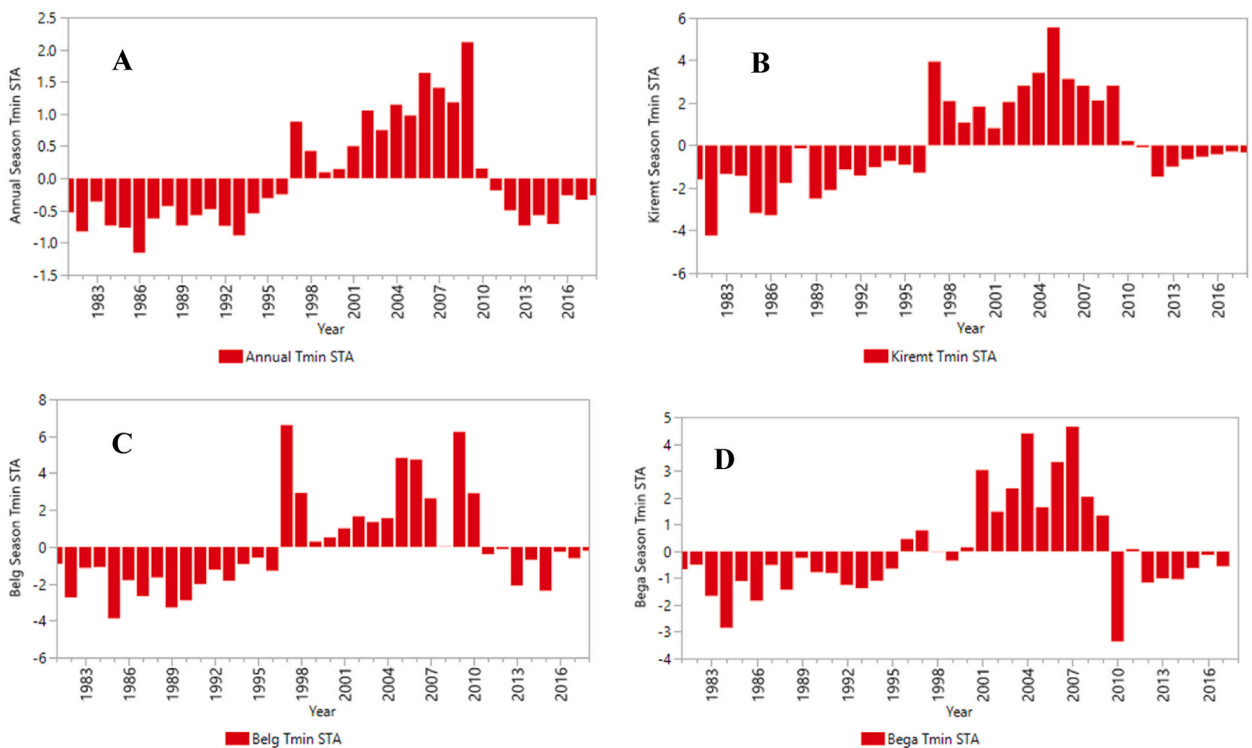

Fig. 13. Long term Tmin anomalies for Annual (a), *Kiremt* (b), *Belg* (c), and *Bega* (d) of Addis Ababa City (1981–2018).
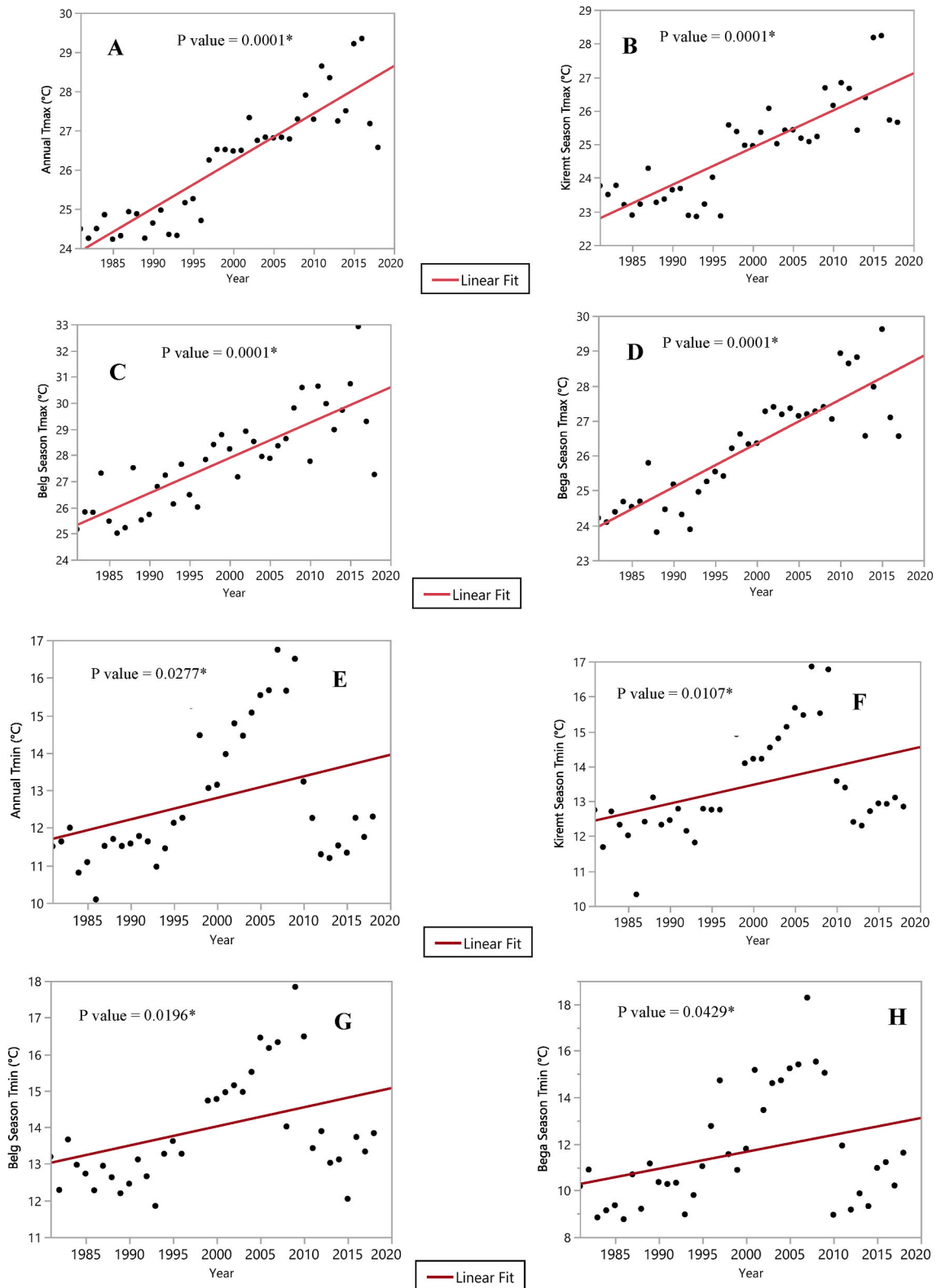
Fig. 14. Average maximum and minimum temperature of Annual (A, E), *Kiremt* (B, F), *Belg* (C, G), and *Bega* (D, H) of Addis Ababa (1981–2018).

Table 1

Average annual and seasonal maximum and minimum temperature record.

mean annual/seasonal Tmax & Tmin (1981–2018)	Degree Celsius (°C)	Year
Highest Annual Tmax	29.35	2016
Highest Annual Tmin	16.75	2007
Lowest Annual Tmax	24.23	1985
Lowest Annual Tmin	10.09	1986
Highest Kiremt Tmax	28.23	2016
Highest Kiremt Tmin	16.86	2007
Lowest Kiremt Tmax	22.85	1993
Lowest Kiremt Tmin	10.33	1986
Highest Belg Tmax	32.92	2016
Highest Belg Tmin	17.84	2009
Lowest Belg Tmax	25.01	1986
Lowest Belg Tmin	11.85	1993
Highest Bega Tmax	29.62	2015
Highest Bega Tmin	18.28	2007
Lowest Bega Tmax	23.81	1988
Lowest Bega Tmin	8.77	1986

Source: ArcGIS statistical analysis result

Table 2

Descriptive statistics of decadal, decadal average maximum/minimum temperature along with variance and standard deviation.

	Observations	Decadal	Mean	Variance	Std.deviation
Maximum temperature (°C)	1981–1990	24.53	22.48	1.63	0.38
	1991–2000	25.33	22.93	1.31	0.31
	2001–2010	26.71	23.98	2.92	0.73
	2011–2018	27.23	24.36	7.38	1.32
Minimum temperature (°C)	1981–1990	11.34	8.91	6.95	0.46
	1991–2000	12.61	9.55	8.89	0.81
	2001–2010	15.16	10.63	6.46	0.78
	2011–2018	11.17	10.41	5.44	0.59

Source: statistical analysis result on ArcGIS

climate in a particular geographic area.

The correlation matrix's result of the Eigenvalue (Table 5) indicated that both the average maximum and minimum temperatures generally show high variation in the maximum and minimum temperatures. The main principal components (PC1, annual Tmax) explain about 65.14% of the total variance. PC2, *Kiremt* (summer) Tmax, reveals the second highest variance, explaining 25.41% of the variation. The third principal component explained 4.1% of the variance. The first two principal components together constituted more than 90% of the variance. Other PCs account for a far smaller percentage of the variance [160]. In this regard, the greater variation in the entire dataset is represented by the first component [166]. The result of the PCA eigenvalue matrix exhibited that PC1 is greater than PC2 and PC2 is higher than PC3. The first three principal components, PC1 (65.14%), PC2 (25.41%), and PC3 (4.11%), as shown in Table 5, provide a good explanation for the influence of eigenvectors on each PCA and its proportion of variance. It is important to denote most of the variation in annual and seasonal maximum and minimum temperature results due to PC1 and PC2.

Comparatively, the annual and seasonal minimum temperatures have shown low variance. Based on the analysis, the first two principal components were the dominant variables that considerably contributed to the increase in temperature in Addis Ababa city. In relation to this, literature denoted that the first PC is linked to heat from the land, the second to heat from the water, and the third to air circulation [182]. Based on this assumption, the PCA analysis result of this study reflected the susceptibility of the city to urban heat island effect.

The analysis result of the cumulative principal components varies from season to season (Table 5) PC1 demonstrated the annual maximum temperature, which has an impact explaining 65.14% of the total variance. PC2 represents the Kiremt season maximum temperature, revealing a total variance of 90.54%. The third principal component, Belg Tmax, explained 94.65% of the total variance. In contrast, the analysis result of the principal components of the minimum temperature for Kiremt (Summer), Belg (Spring), and Bega (Winter) showed a cumulative variance of almost 100%. Thus, it is possible to conclude that the combination of the first two PCs highly influenced the change in temperature in Addis Ababa city.

As shown in Table 6, in PC4, the effect of the annual maximum and minimum temperature was dominant, while in PC3, the Kiremt (summer) temperature maximum and minimum had a strong impact. In PC2, Belg (spring) and Bega (winter) temperatures had a moderate impact. Both the annual and seasonal maximum and minimum temperatures have a low impact on PC1.

Fig. 17 revealed the percentage of each dimension's (PCs) contribution to the variance of both maximum and minimum temperature. As the scree plot depicts, there are eight dimensions that represent both the maximum and minimum temperature of both annual and seasonal. Dim-1 and Dim-5 represented annual Tmax and Tmin; Dim-2 and Dim-6 indicated Kiremt season Tmax and Tmin; Dim-3 and Dim-7 reflect Belg season Tmax and Tmin; Dim-4 and Dim-8 are attributed to Bega season Tmax and Tmin, respectively. Dim-1
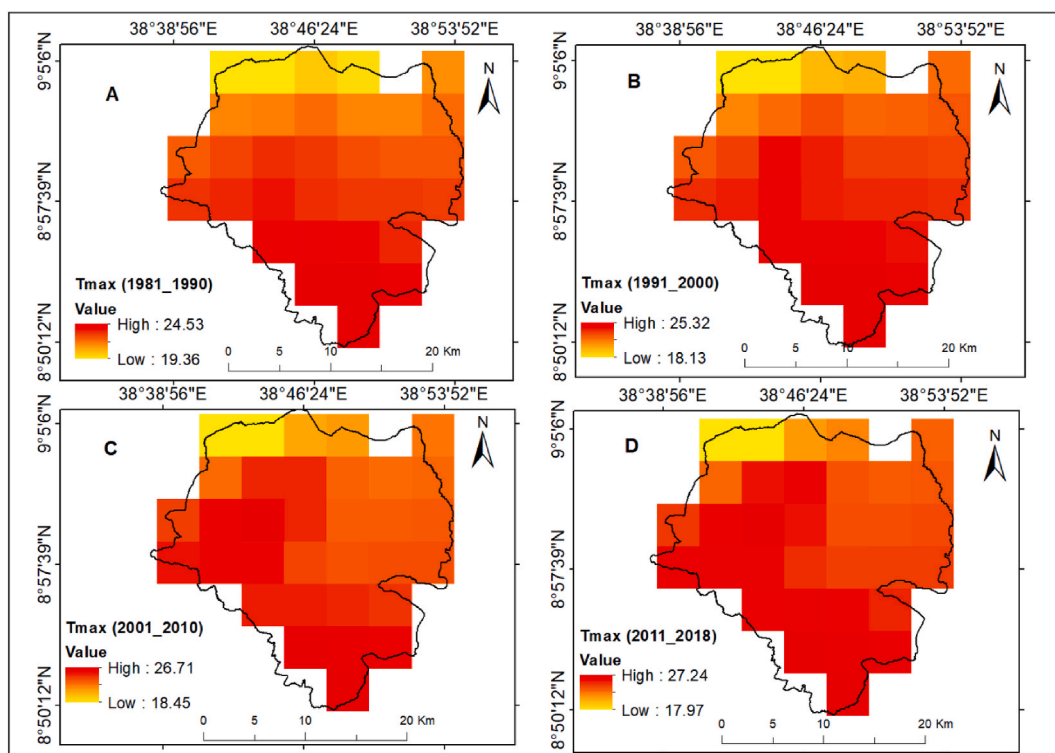
Fig. 15. Portrays the average decadal maximum temperature of Addis Ababa for the year (A) 1981–1990, (B) 1991–2000, (C) 2001–2010 and (D) 2011–2018.

(annual Tmax) and Dim-2 (Kiremt Tmax) explained a variance of 65.1% and 25.4%, respectively. While the least contribution was attributed to *Bega* (winter) Tmin (0.1%). In this case, the scree plot analysis result is consistent with the eigenvalue matrix result displayed in the table shown (Table 6).

The variable graph (18 left A) demonstrated the correlation between the maximum and minimum temperature on the principal components, PC1 and PC2. Generally, the result implies that there is a positive correlation among the different variables. Both plots (Fig. 18 right B) illustrated that Dim-1 (PC1) has 65.1% variation, whereas Dim-2 (PC2) contains 25.4% variation. In addition, the analysis results further exhibited that the annual Tmax and annual Tmin (green color) are highly correlated. While Kiremt Tmax and Tmin (light gray color) were moderately correlated, a negative correlation (red color) was found between Belg Tmax and Belg Tmin; the same is true for Bega Tmax and Bega Tmin. This implies that the average annual maximum and minimum temperature played a significant role in the increase of Addis Ababa City's temperature.

Fig. 19 left A and right B reveal the contribution of each variable for the first two dimensions (PCs). Among the various seasons, Kiremt Tmin, Annual Tmax, Annual Tmin, and Kiremt Tmax contributions were the highest Particularly, Kiremt and Annual Tmax played significant contributors for both dimensions (Fig. 19 A and B). On the other hand, the contribution of variables to dimension 2 was Bega Tmin, Annual Tmin, Kiremt Tmax, and Annual Tmax. Bega Tmin and Annual Tmin were the greatest as compared to others. Similarly, the figure on the right side also explains the contribution of each variable to each dimension (PCs). As shown in the figure on the right, all the variables contribute to dimension 1 (PC1) in different degrees. Annual Tmax and Kiremt Tmin contributed the most which is >0.7%. It was followed by Kiremt and Bega Tmax, annual Tmin, and Belg Tmin. The least contribution comes from Bega Tmin. Similarly, all the different variables at varying degrees contributed to dimension 2 (PC2). However, the greatest contribution came from annual Tmax, Kiremt Tmax, Annual Tmin, and Bega Tmin. For the remaining dimensions, the contribution of each variable was insignificant.

3.8.2. Monthly PCA analysis result

Table 7 highlights the monthly correlation matrix results of the three PCs and their respected results of eigenvalue matrix. The eigenvalue matrix stipulated that the first two principal components (PC1 and PC2) account for 100% of the total data variance (Fig. 20-left A). Especially, PC1 immensely contributed (66.8%) to the variance of monthly temperature. While PC3 has insignificant contribution (0.3%). When examining the individual contribution (Fig. 20-right B) for Dim-1-2 (PC1 and PC2), the months of August, May, July, and March are the largest contributors that highly influence the variability of monthly temperature in the period of concern over the study area.

Evidently, as the correlation matrix (Fig. 21, left A and right B) depicts, the average and maximum temperatures have a strong influence on the variables related to monthly temperature, and they are highly correlated. Contrary to this, the influence of the
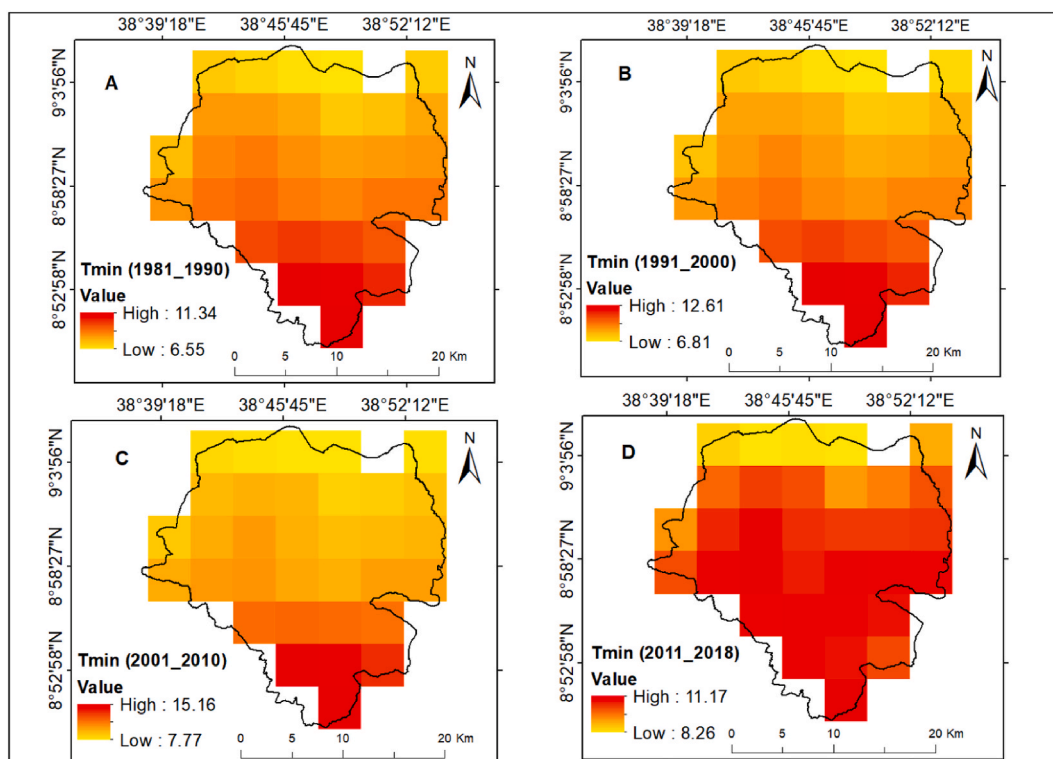
Fig. 16. Demonstrates the average decadal minimum temperature of Addis Ababa for the year (A) 1981–1990, (B) 1991–2000, (C) 2001–2010 and (D) 2011–2018.

Table 3
MMK trend analysis of average annual and seasonal maximum and minimum temperature (1981–2018) in Addis Ababa.

Seasons	Kendall's tau	P-value	Trend	Significant	Sen's slope (°C/year)	Var(s)	Test statistics (Z)
Annual Tmax	0.73	0.0001	Increasing	Significant	0.12	1842.69	11.97
Annual Tmin	0.32	0.0056	Increasing	Significant	0.064	6544.77	2.77
Kiremt Tmax	0.61	0.0001	Increasing	Significant	0.11	1963.22	9.70
Kiremt Tmin	0.33	0.0032	Increasing	Significant	0.052	6295.49	2.95
Belg Tmax	0.65	0.0001	Increasing	Significant	0.14	544.42	5.76
Belg Tmin	0.30	0.0050	Increasing	Significant	0.049	5707.15	2.81
Bega Tmax	0.67	0.0001	Increasing	Significant	0.126	1880.86	10.95
Bega Tmin	0.27	0.0130	Increasing	Significant	0.072	5794.46	2.48

Source: Rstudied Modified Menn-Kendell test Significant at $\alpha = 0.05$

minimum temperature was insignificant. As the correlation result displays, the level of variation of Dim-1 (PC1) and Dim-2 (PC2) was 66.8% and 33%, respectively.

It is important to note that PC1 is higher than PC2. This signifies that 99.8% of the variation in monthly maximum and minimum temperature was due to PC1 and PC2.

Fig. 22, left A and right B, show the analysis result of the monthly contributions for Dim-1 and Dim-2, revealing that the maximum and average temperature were by far the largest contributors for Dim-1 (PC1). While monthly Tmin is the single most important contributor for Dim-2 (PC2). This is also supported by the analysis results under Table, which reveal that Tmax and the monthly average were the principal components of PC1 and PC2.

3.9. T-test analysis of Tmax and Tmin

Tables 8 and 9 show the t.test analysis result for maximum and minimum temperature of the study period. The mean annual max temperature (M = 26.16, SD = 1.499, n = 38) was hypothesized to be greater than the mean annual min temperature (M = 12.767, SD = 1.787, n = 38). The difference was significant t (74) = 1.99, $p = 0.000$ (1 tail). This means a highly statistically significant result. As the p-value is significantly lower than (1.94 × 10^-48), it is considered that the findings are significant.

Table 4
MMK trend analysis of monthly Tmax and Tmin (1981–2018) in Addis Ababa City.

Month	Mean's value	Kendall's tau	P-value	Trend	Significant	Sen's slope (mm/year)	Var(s)	Test statistics (Z)
January Tmax	26.09	0.64	0.0001	Increasing	Significant	0.124	1346.13	12.32
January Tmin	10.88	0.21	0.0523	Increasing	Insignificant	0.061	5510.50	1.94
February Tmax	26.79	0.60	0.0001	Increasing	Significant	0.152	1581.95	10.56
February Tmin	12.14	0.16	0.046	Increasing	Significant	0.053	3057.49	2.00
March Tmax	27.59	0.59	0.0001	Increasing	Significant	0.135	586.79	17.17
March Tmin	13.12	0.20	0.0073	Increasing	Significant	0.046	2799.69	2.68
April Tmax	27.03	0.58	0.0001	Increasing	Significant	0.162	510.81	17.96
April Tmin	14.01	0.30	0.0029	Increasing	Significant	0.063	5092.98	2.97
May Tmax	27.52	0.56	0.0001	Increasing	Significant	0.122	988.59	12.47
May Tmin	14.33	0.34	0.0019	Increasing	Significant	0.076	5781.41	3.10
June Tmax	26.11	0.52	0.0001	Increasing	Significant	0.108	1212.11	10.51
June Tmin	13.53	0.35	0.0011	Increasing	Significant	0.066	5497.75	3.26
July Tmax	23.79	0.58	0.0001	Increasing	Significant	0.113	2326.45	8.50
July Tmin	13.39	0.40	0.0000	Increasing	Significant	0.067	4945.65	3.98
August Tmax	23.37	0.52	0.0001	Increasing	Significant	0.082	1510.38	9.366
August Tmin	13.36	0.33	0.0023	Increasing	Significant	0.049	5575.42	3.05
September Tmax	24.65	0.67	0.0001	Increasing	Significant	0.119	1479.89	12.17
September Tmin	13.06	0.22	0.0585	Increasing	Insignificant	0.041	6455.18	1.89
October Tmax	25.59	0.65	0.0001	Increasing	Significant	0.126	1603.57	11.44
October Tmin	11.87	0.28	0.0075	Increasing	Significant	0.096	5271.96	2.67
November Tmax	25.55	0.66	0.0001	Increasing	Significant	0.134	1489.56	11.92
November Tmin	11.29	0.32	0.0004	Increasing	Significant	0.109	4128.33	2.84
December Tmax	25.33	0.59	0.0001	Increasing	Significant	0.097	5120.52	5.52
December Tmin	10.70	0.23	0.0140	Increasing	Significant	0.095	4242.22	2.46

Source: Modified Menn-Kendell test result in R Significant at α = 0.05

Table 5
Eigen values of the correlation matrix (1981–2018).

Seasons	Annual Tmax	Kiremt Tmax	Belg Tmax	Bega Tmax	Annual Tmin	Kiremt Tmin	Belg Tmin	Bega Tmin
Tmax, Tmin	PC1	PC2	PC3	PC4	PC5	PC6	PC7	PC8
Eigenvalue	5.21	2.03	0.33	0.28	0.08	0.05	0.02	0.01
% Variance	65.14	25.41	4.11	3.45	1.03	0.57	0.24	0.06
% cumulative variance	65.14	90.54	94.65	98.10	99.13	99.70	99.94	100
Standard deviation	2.28	1.43	0.57	0.53	0.29	0.21	0.14	0.07

Source: PCA analysis in R studio

Table 6
The principal components elements of annual and seasonal (1981–2018).

Annual/seasonal Tmax	PC1	PC2	PC3	PC4
Annual Tmax	0.52	0.06	−0.00	**0.85**
Kiremt Tmax	0.51	−0.07	**0.80**	−0.31
Belg Tmax	0.48	**0.70**	−0.38	−0.35
Bega Tmax	0.48	**−0.70**	−0.47	−0.25
Annual/seasonal Tmin	PC1	PC2	PC3	PC4
Annual Tmin	0.52	−0.04	0.10	**0.85**
Kiremt Tmin	0.52	0.03	**0.75**	−0.40
Belg Tmin	0.48	**0.71**	−0.47	−0.21
Bega Tmin	0.48	**−0.71**	−0.44	−0.28

Source: PCA analysis result in R studio. Bold values represent statistically significant impact (no impact at 0.0–0.2; low impact 0.2–0.4; moderate impact 0.4–0.7; high impact 0.7–0.9; and very strong impact 0.9–1.0 [173]).

4. Discussion

Globally, the mean surface temperature by the end of the 21st century is anticipated to increase from 0.3 °C to 4.8 °C, with consequent drought, flooding, and heatwaves expected to become more frequent [44]. The global surface temperature in the first two decades of the 21st century (2001–2020) was 0.99 °C higher than 1850–1900 [183]. On top of that, the United Nations Development Program [UNDP] country profile shows that from 1960 to 2006, there was an average annual temperature increase of 1.3 °C, 0.28 °C per decade [184]. In the context of Addis Ababa, a study by Ref. [58] noted that changes in minimum and maximum temperature over Addis Ababa city are evaluated using high resolution NIRRHaGEM-AO simulations for future projections under prepresentative
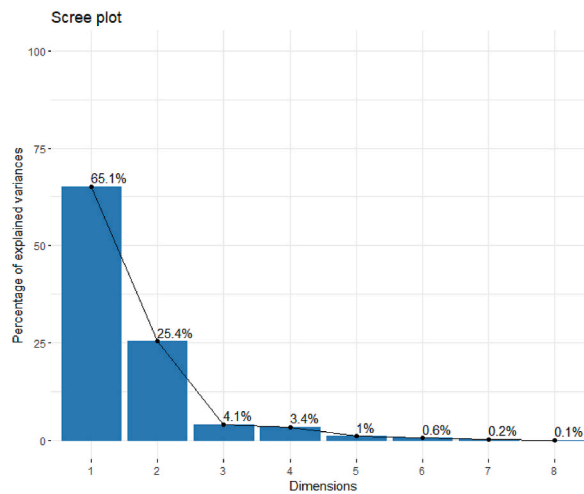
Fig. 17. Portrays the percentage of each dimension contribution for the variance.
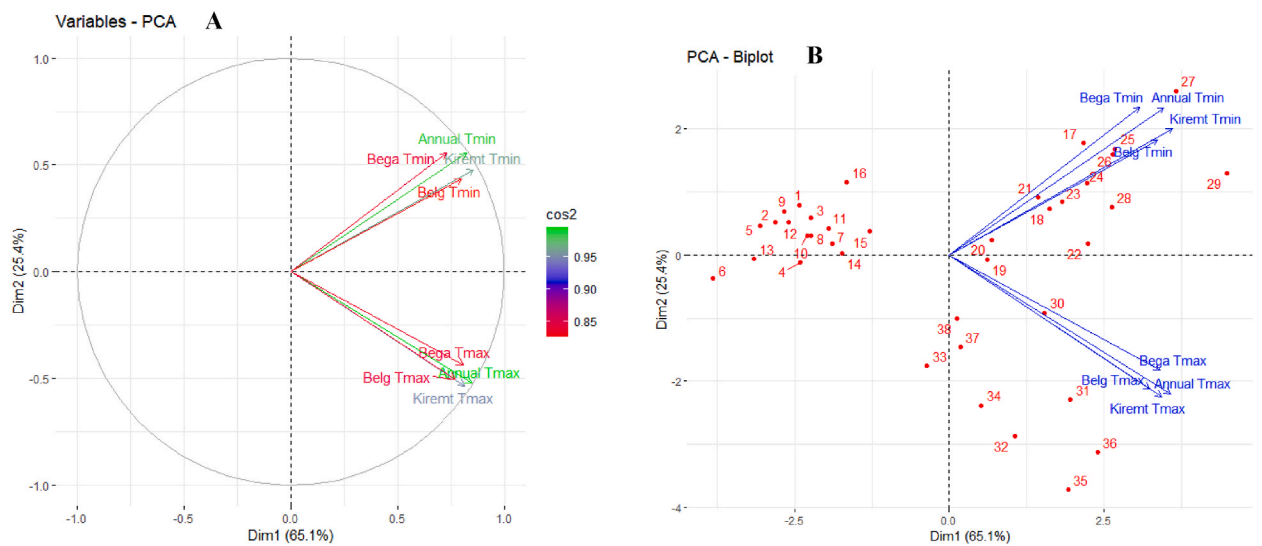

Fig. 18. Illustrates the correlation of variable to PCA (left A) and PCA-Biplot (right B).

concentration pathways (RCP8.5) and gridded observations. The result indicated that both the minimum and maximum temperature getting warmer between 1950 and 2000.

In addition [48], carried out a study in Addis Ababa by taking two main meteorological stations, i.e., Entoto and Bole. The result of the study signified that there was a significant increase in the average annual temperature for Bole station, while for Entoto it was insignificantly increased. Similarly, between 1960 and 2006, Addis Ababa's average annual temperature increased by 1.3 °C [184]. The findings of this study is comparable with the previous research which designated that over the last 38 years (1981–2018), the average decadal maximum and minimum temperature increased by 1.88 and 1.72 °C, respectively. Comparatively, all the previous studies covered a different time period, however, the findings of their study were conclusively consistent with the results of this research, which all underscore an increase of temperature in Addis Ababa.

Moreover [53], used data from Entoto and Addis Ababa Observatory stations to statistically downscale the daily maximum and minimum temperature at 30-year intervals. Based on the results, the Addis Ababa Observatory experienced maximum temperature rises between 2020 and 2080, ranging from 0.9 °C (RCP4.5) to 2.1 °C (CGCM3A2). It is predicted that the minimum temperature will rise by 1.0 °C in 2080 and 0.3 °C in 2020. The study underlines that future scenarios predict that both the minimum and maximum temperatures will increase. All the previous studies reported that the historical trend of temperature and future projections revealed that there was an increase in maximum and minimum temperature in the city. Their findings were aligned with the findings of this research, which found that there was a significant upward trend in both the annual and seasonal maximum and minimum temperatures in the area of concern.
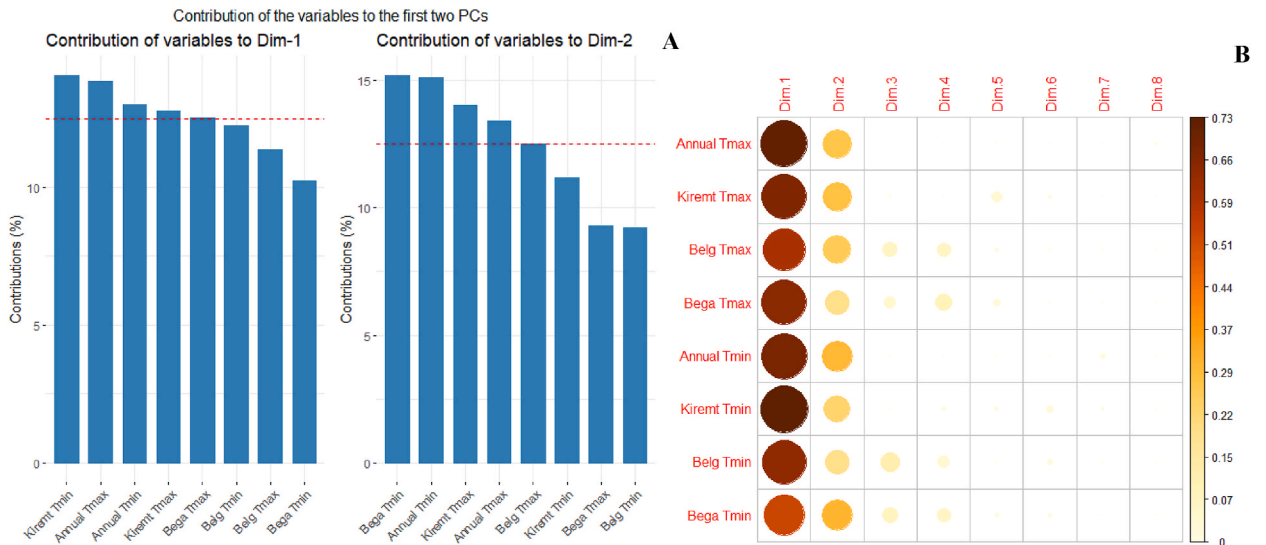
Fig. 19. Shows the contribution of each variable for the different PCs (left A and right B).

Table 7
The monthly principal component elements and Eigen values matrix (1981–2018).

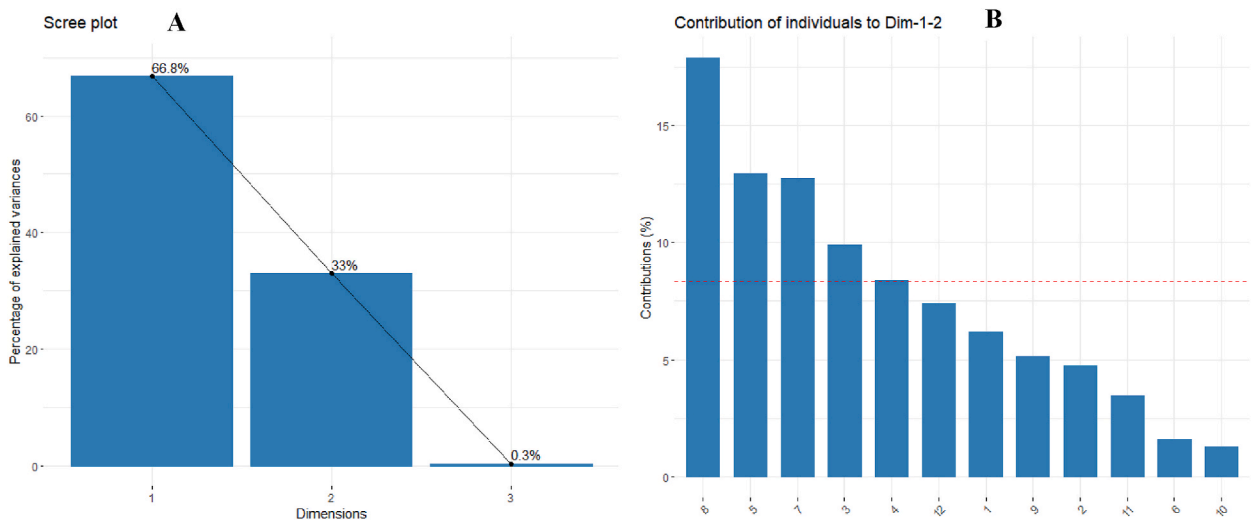| Monthly/components	PC1	PC2	PC3
Tmax	−0.70	0.04	0.71
Tmin	−0.12	−0.10	−0.06
Average	−0.70	0.13	−0.70
Eigenvalue	2.00	0.99	0.01
% variance	0.67	0.33	0.00
% cumulative variance	0.67	0.10	1.00
Standard deviation	1.42	0.99	0.10

Source: analysis result in R studio

Fig. 20. Depicts the percentage of explained variance (left A) and contribution of individuals to Dim-1-2 (right B).

As literature pointed out, the possible causes of the observed increase in temperature largely are attributed to anthropogenic factors. In relation to this, the recent IPCC report noted that the increase in mean and extreme temperature trends across Africa is attributable to human-caused [185]. Extreme weather changes in Addis Ababa were observed due to changes in climate [48]. The other reasons that could contribute to the rise of the city's temperature over the course of the study period would be largely associated
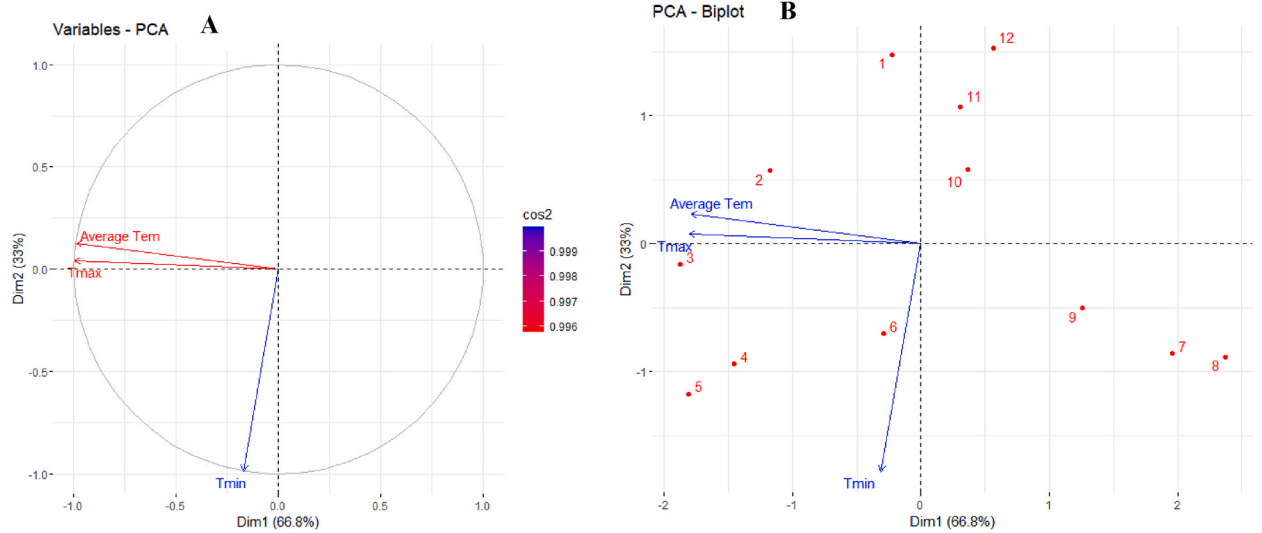
Fig. 21. Portrays correlation circles of monthly Tmax, Tmin, and Average (left A) and Biplot of the same variables (right B).
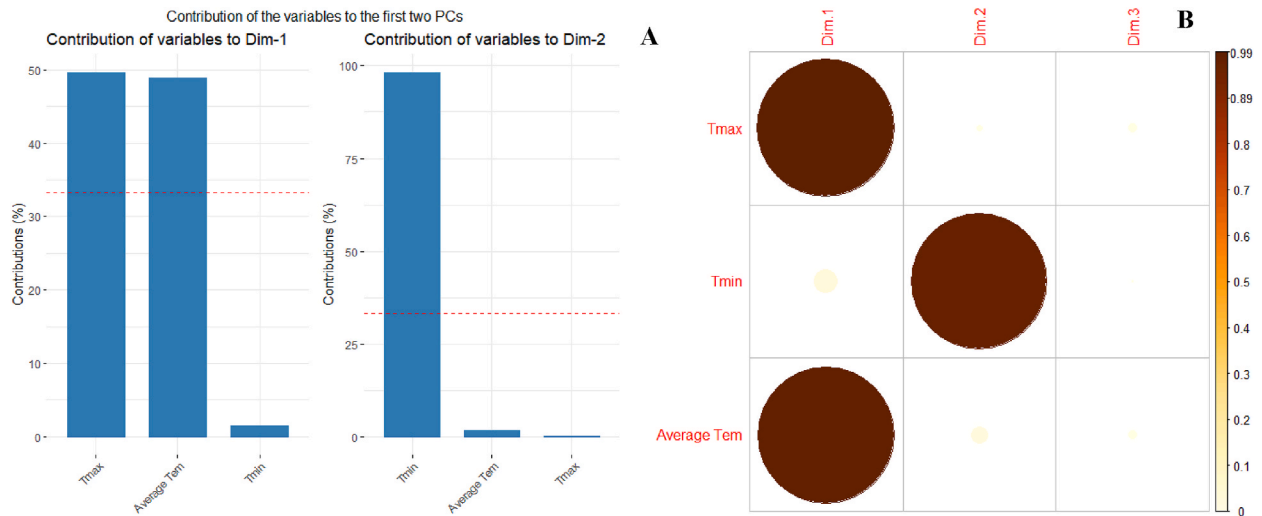

Fig. 22. Illustrates in the contribution of variables for the first two PCs (left A and right B).

Table 8
T-test for annual maximum and minimum temperature (1981–2018).

Average Annual Tmax		Average Annual Tmin	
Mean	**26.164231**	**Mean**	**12.7671173**
Standard Error	0.2432331	Standard Error	0.289887436
Median	26.505108	Median	12.06654
Mode	#N/A	Mode	#N/A
Standard Deviation	**1.4993893**	**Standard Deviation**	**1.786986171**
Sample Variance	2.2481684	Sample Variance	3.193319576
Kurtosis	−0.857854	Kurtosis	−0.555415339
Skewness	0.3116161	Skewness	0.828831386
Range	5.1177	Range	6.655266667
Minimum	24.228525	Minimum	10.0909
Maximum	29.346225	Maximum	16.74616667
Sum	994.24078	Sum	485.1504575
Count	**38**	**Count**	**38**

Table 9
T-test: two-sample assuming equal variances.

	Mean Annual Tmax	Mean Annual Tmin
Mean	**26.16423**	**12.7671173**
Variance	2.248168	3.193319576
Observations	**38**	**38**
Pooled Variance	2.720744	
Hypothesized Mean Difference	0	
df	**74**	
t Stat	35.40334	
P(T<=t) one-tail	**1.94E-48**	
t Critical one-tail	1.665707	
P(T ≤ t) two-tail	3.88E-48	
t Critical two-tail	1.992543	

Source: statistical analysis result using origin software.

with urbanization. Over the last three decades, the magnitude of urbanization and economic development have led to an unprecedented rate of increase in the urban population in the city. The population of Addis Ababa accounts for 3.6% of the national population and 18% of Ethiopia's urban population, with an annual growth rate of 2.1% [59]. Specially, the population over the last decade has been alarmingly increasing due to economic and political reasons. This reflects that there has been a high rate of urbanization driven by overwhelming population growth. As a result, many landforms that were covered by dense forest, vegetation, including public spaces, and other natural features, with the growth of population and urbanization, transformed into built-up areas, industries, and high-rise buildings. This is largely a contributing factor for the escalation of the city's temperature. Of course, this has to be supported objectively with empirically evidence with field data, it also requires further investigation and could be considered a potential research area, including scenarios such as people's perceptions on the observed changes of temperature in the city.

Making resilient cities resilient against man-made and natural disasters continues to be a serious concern for both developed and developing nations [186]. The United Nations report outlines a number of Sustainable Development Goals [187]. The SDG 11 focuses on Sustainable Cities and Communities, i.e., making cities and human settlements inclusive, safe, resilient, and sustainable. The primary goal of SDG 13 is to increase all nations' resilience and capacity for adaptation to climate related threats. Both goals are highly linked with the intent of this study. Cities like Addis Ababa, where there is a growing concern over the rise of temperature and associated environmental repercussions. Due attention has to be given by the city administration towards the realization of these development goals and to creating a more vibrant habitable, and environmentally friendly living environment. In relation to that, the Addis Ababa city administration could consider the garden city concept [188], integrating with city's urban planning and design framework in such a way that the construction of new settlements surrounded by green areas. Considering the city not only to have an ecological advantage but also economic and cultural advantages.

The study recommends mitigation and adaptation measures in order to cope with the warming effect induced by temperature increases in Addid Ababa. For this reason, cooperation and integration of the different government institutions working in the areas of climate change, forestry, environmental protection and preservation, and natural disaster management etc. Would be imperative in order to effectively monitor the environment and realize a sustainable, healthy, livable, and resilient urban environment. Additionally, measures such as city-wide green space initiative have to be practiced in the major corridors of the city, including at the neighborhood, village level, and private houses. This can be achieved with the support of indigenous knowledge in identifying, selecting, and plating fast growing trees/seeds that are suitable for the local climate conditions, soil, and with minimal environmental risk. In that regard, the local communities need to have the mandate and ownership in cultivating, monitoring, and managing the plated seeds/trees in their immediate surrounding environment. In connection with this, one initiative could be converting pocket spaces that have been used as a place to dispose trash into gardens.

Raising awareness among the people would be the number one priority. In cities like Addis Ababa, the majority of the people have low awareness on the growing impacts of global warming at the local level. This requires the concerted efforts of different stakeholders, including the government, non-government organizations, investors, media, and the residents of the city. The people need to understand the ecological benefits of keeping the city clean and green for a healthy, environmentally friendly, and habitable environment. With the motto of plating a single tree, can matter for a healthier lifestyle and for the better future of our children. In order to bring the desired change and elevate people's awareness among the wider population, it requires a policy directive.

The consistent temperature rise observed in Addis Ababa has far-reaching implications. It can impact various aspects of the environment and society, including water resources, urban agriculture, and urban planning. The warming trend poses challenges for water availability and urban infrastructure. The presence of high urban structures in the city, such as building, roads, and other infrastructures largely absorb the atmospheric temperature during the day and reemits this energy towards the environment during night. This largely contributed for the increase of temperature and result in environmental and health related consequences such as urban heat island effect. Thus, the current urban planning and design has to take into consideration in addressing this matter. As a policy, the buildings constructed in the city have to be ecologically and environmentally friendly, and greenery buildings have to be implemented and largely practiced within the city. Furthermore, the study underscores the importance of ongoing climate monitoring and adaptation efforts to address the consequences of rising temperatures.

5. Conclusion

The study conducted an in-depth analysis of temperature variations in Addis Ababa, Ethiopia, over a 38-year period from 1981 to 2018. The investigation has covered various aspects, including monthly fluctuations, annual, seasonal patterns, and decadal levels. Coefficients of variation, standardized anomaly index, Modified Menn-Kendall test, principal component analysis, and *t*-test were employed and analyzed using geospatial technologies, "R" programming and statistical software. The findings of this comprehensive study unveiled a significant spatial and temporal variations in temperature within Addis Ababa. The key findings were:

- Temperature variations exhibited relatively moderate coefficients of variation (CV) for both maximum and minimum temperature. The lowest variability observed during the *Belg* (Spring) season.
- Monthly temperature analysis highlighted a significant fluctuation, with March being the hottest month and December the coolest.
- The coefficient of variation remained below 20% for maximum temperatures in all months, while minimum temperatures exhibited slightly higher variability in November, December, and January.
- The study identified a warming trend in maximum temperatures across all seasons from 2011 to 2018. This warming effect was statistically significant, with strong correlations observed between time and increasing maximum temperature anomalies.
- Trend analysis confirmed a positive trend in both annual and seasonal maximum and minimum temperatures over the study period.
- Maximum temperature demonstrated a more pronounced increase, with statistical significance particularly notable in the *Belg* season.
- Decadal analysis revealed a steady rise in maximum temperatures throughout the study period, with an overall increase of 2.7 °C.
- The Modified Mann-Kendall and Sen's slope estimator tests provided further evidence of an upward trend in both maximum and minimum temperatures.
- Based on the results of the PCA analysis, it was determined that PC1 (mean annual Tmax) and PC2 (mean Kiremt Tmax) accounted for almost 90% of the variation in temperature.
- The *t*-test analysis further proofed that there was a significant increase in the annual and seasonal maximum and minimum temperatures.

Data availability

Data will be made available on request.

Funding statement

CRediT authorship contribution statement

Esubalew Nebebe Mekonnen: Writing – original draft, Software, Methodology, Formal analysis, Conceptualization. **Aramde Fetene:** Writing – review & editing, Validation, Supervision. **Ephrem Gebremariam:** Writing – review & editing, Supervision.

Declaration of competing interest

The authors declare that they have no known competing financial interests or personal relationships that could have appeared to influence the work reported in this paper.

Acknowledgments

References

[1] W.N. Adger, P.M. Kelly, Social Vulnerability to Climate Change and the Architecture of Entitlements, 1999, pp. 253–266.
[2] Q. Guo, Z. He, Z. Wang, Long-term projection of future climate change over the twenty-first century in the Sahara region in Africa under four Shared Socio-Economic Pathways scenarios, Environ. Sci. Pollut. Res. 30 (9) (2023) 22319–22329, https://doi.org/10.1007/s11356-022-23813-z.
[3] Y.A. Tessema, C.S. Aweke, G.S. Endris, "Understanding the process of adaptation to climate change by small-holder farmers : the case of east Hararghe Zone, Ethiopia," 1 (May 2016) (2013), https://doi.org/10.1186/2193-7532-1-13.
[4] P.B.I. Akponikpè, P. Johnston, E.K. Agbossou, Farmers' perception of climate change and adaptation strategies in Sub- Saharan West-Africa, 2nd Int. Conf. Clim. Sustain. Dev. semi-arid Reg. 15 (January 2015) (2010).
[5] C.D. Butler, Climate change, health and existential risks to civilization: a comprehensive review (1989–2013), Int. J. Environ. Res. Publ. Health 15 (10) (2018), https://doi.org/10.3390/ijerph15102266.
[6] IPCC, Climate Change 2021 The Physical Science Basis WGI 34 (2) (2021).

[7] M.B. Ware, T. Matewos, M. Guye, A. Legesse, Y. Mohammed, Spatiotemporal variability and trend of rainfall and temperature in Sidama Regional State, Ethiopia, Theor. Appl. Climatol. (2023) 0123456789, https://doi.org/10.1007/s00704-023-04463-8.

[8] G.A. Bogale, T.T. Tolossa, Climate change intensification impacts and challenges of invasive species and adaptation measures in Eastern Ethiopia, Sustain. Environ. 7 (1) (2021), https://doi.org/10.1080/23311843.2021.1875555.

[9] P. Forster, et al., Changes in Atmospheric Constituents and in Radiative Forcing, 2007 [Online]. Available: http://hero.epa.gov/index.cfm?action=reference. details&reference_id=92936.

[10] IPCC, Managing the Risks of Extreme Events and Disasters to Advance Climate Change Adaptation, 2012, https://doi.org/10.1017/cbo9781139177245.

[11] Oxfam, Oxfam Media Briefing - A Climate in Crisis, 2017 no. April, p. 27 April, https://www-cdn.oxfam.org/s3fs-public/mb-climate-crisis-east-africa-drought-270417-en.pdf.

[12] IPCC, Climate change 2021 the physical science basis, Work. Gr. I Contrib. to Sixth Assess. Rep. Intergov. Panel Clim. Chang. 34 (2) (2021), https://doi.org/10.3724/sp.j.7103161536. F0003–F0003.

[13] IPCC, *Summary for Policymakers*: Climate Change 2022_ Impacts, Adaptation and Vulnerability_Working Group II Contribution to the Sixth Assessment Report of the Intergovernmental Panel on Climate Change, August, 2022, https://doi.org/10.1017/9781009325844.Front.

[14] J.V. Henderson, A. Storeygard, U. Deichmann, Is Climate Change Driving Urbanization in Africa?, 2014.

[15] IPCC, Climate change 2007 The Physical Science Basis 59 (8) (2007), https://doi.org/10.1256/wea.58.04.

[16] IPCC, The IPCC's Fifth Assessment Report What's in it for Africa?, 2014.

[17] A.S. Belay, et al., Evaluation and application of multi-source satellite rainfall product CHIRPS to assess spatio-temporal rainfall variability on data-sparse western margins of Ethiopian highlands, Rem. Sens. 11 (22) (2019) 1–22, https://doi.org/10.3390/rs11222688.

[18] IPCC, Climate Change 2022 Impacts, Adaptation and Vulnerability Summary for Policymakers, Implement. a US Carbon Tax Challenges Debates, 2022, pp. xxiii–xxxiii, https://doi.org/10.4324/9781315071961-11.

[19] O. Hoegh-Guldberg, et al., The human imperative of stabilizing global climate change at 1.5°C, Science 365 (6459) (2019), https://doi.org/10.1126/science.aaw6974.

[20] M.A. Hassaan, M.A. Abdrabo, P. Masabarakiza, GIS-based model for mapping malaria risk under climate change case study: Burundi, J. Geosci. Environ. Protect. 5 (11) (2017) 102–117, https://doi.org/10.4236/gep.2017.511008.

[21] K. Mwangi, F. Mutua, Modeling Kenya's vulnerability to climate change – a multifactor approach (pdf download available), Thesis MSc. Geospatial Inf. Syst. Remote Sensing 4 (6) (2015) 12–19 [Online]. Available: https://www.researchgate.net/publication/279885203_Modeling_Kenya's_Vulnerability_to_Climate_Change_-_A_Multifactor_Approach.

[22] I. Niang, O.C. Ruppel, A.E. Abdrabo, C. Lennard, J. Padgham, P. Urquhart, Chapter 22 Africa, in: Climate Change 2014: Impacts, Adaptation, and Vulnerability. Part B: Regional Aspects. Contribution of Working Group II to the Fifth Assessment Report of the, 2014.

[23] S. Pauleit, et al., Urban Vulnerability and Climate Change in Africa: A Multidisciplinary Approach, vol. 4, 2015 [Online]. Available: http://www.springer.com/de/book/9783319039848.

[24] World Bank, AFRICA REGION Making Development Climate Resilient: A World Bank Strategy for Sub-saharan Africa, 2009 no. 46947, https://openknowledge.worldbank.org/bitstream/handle/10986/3211/469470ESW0Whit0t20100Full0vNoImages.pdf?sequence=1&isAllowed=y.

[25] B.A. Abebe, B. Grum, A.M. Degu, H. Goitom, Spatio-temporal rainfall variability and trend analysis in the Tekeze-Atbara river basin, northwestern Ethiopia, Meteorol. Appl. 29 (2) (2022) 1–17, https://doi.org/10.1002/met.2059.

[26] D. Ayalew, K. Tesfaye, G. Mamo, B. Yitaferu, W. Bayu, Variability of rainfall and its current trend in Amhara region, Ethiopia 7 (10) (2012) 1475–1486, https://doi.org/10.5897/AJAR11.698.

[27] N. Stern, The economics of climate change: the stern review, Econ. Clim. Chang. Stern Rev. 9780521877 (2007) 1–692, https://doi.org/10.1017/CBO9780511817434.

[28] Climate resilient green economy, "green economy strategies,", Green Econ. Oppor. Challenges (2011) 81–99, https://doi.org/10.4324/9781003206729-4.

[29] S.H. Gebrechorkos, S. Hülsmann, C. Bernhofer, Changes in temperature and precipitation extremes in Ethiopia, Kenya, and Tanzania, Int. J. Climatol. 39 (1) (2018) 18–30, https://doi.org/10.1002/joc.5777.

[30] D. Conway, E.L.F. Schipper, Adaptation to climate change in Africa: challenges and opportunities identified from Ethiopia, Global Environ. Change 21 (1) (2011) 227–237, https://doi.org/10.1016/j.gloenvcha.2010.07.013.

[31] E. Ludi, et al., Preparing for the Future? Understanding the Influence of Development Interventions on Adaptive Capacity at Local Level in Ethiopia: Africa Climate Change Resilience Alliance (ACCRA) Ethiopia Synthesis Report, 2011 no. January.

[32] G.G. Cherie, Climate Change Impact Assessment of Dire Dam Water Supply, 2015, pp. 1–102. March,.

[33] G.T. Diro, A.M. Tompkins, X. Bi, Dynamical downscaling of ECMWF ensemble seasonal forecasts over East Africa with RegCM3, J. Geophys. Res. Atmos. 117 (16) (2012) 1–20, https://doi.org/10.1029/2011JD016997.

[34] D.P. Rowell, B.B.B. Booth, S.E. Nicholson, P. Good, Reconciling past and future rainfall trends over East Africa, J. Clim. 28 (24) (2015) 9768–9788, https://doi.org/10.1175/JCLI-D-15-0140.1.

[35] Z. Dendir, B.S. Birhanu, Analysis of observed trends in daily temperature and precipitation extremes in different agroecologies of gurage zone, southern Ethiopia, Adv. Meteorol. 2022 (2022), https://doi.org/10.1155/2022/4745123.

[36] D.A. Tofu, M. Mengistu, Observed time series trend analysis of climate variability and smallholder adoption of new agricultural technologies in west Shewa, Ethiopia, Sci. African 19 (2023) e01448, https://doi.org/10.1016/j.sciaf.2022.e01448.

[37] UN-Habitat, Envisaging the Future of Cities, 2022.

[38] UN Habitat, *Global Report On Human Settlements 2011: Cities and Climate Change*, 2011.

[39] UN, "Cities and climate change: national governments enabling local action,", Change (2014) 276 [Online]. Available: https://www.oecd.org/env/cc/Cities-and-climate-change-2014-Policy-Perspectives-Final-web.pdf%5Cn.

[40] G.L. Feyisa, K. Dons, H. Meilby, Efficiency of parks in mitigating urban heat island effect: an example from Addis Ababa, Landsc. Urban Plann. 123 (2014) 87–95, https://doi.org/10.1016/j.landurbplan.2013.12.008.

[41] World Bank, Guide to climate change adaptation in cities, Guid. to Clim. Chang. Adapt. Cities (2011), https://doi.org/10.1596/27396.

[42] A. Averchenkova, K.E. Gannon, P. Curran, Governance of Climate Change Policy: A Case Study of South Africa, November, 2019, pp. 1–40, https://doi.org/10.13140/RG.2.2.23403.49443.

[43] N. Sibiya, M. Sithole, L. Mudau, M.D. Simatele, Empowering the Voiceless: securing the participation of marginalised groups in climate change governance in South Africa, Sustain. Times 14 (12) (2022), https://doi.org/10.3390/su14127111.

[44] IPCC, Climate Change 2014 Synthesis Report 9781107025 (2014), https://doi.org/10.1017/CBO9781139177245.003.

[45] D. Jacob, et al., EURO-CORDEX: new high-resolution climate change projections for European impact research, Reg. Environ. Change 14 (2) (2014) 563–578, https://doi.org/10.1007/s10113-013-0499-2.

[46] G. Krinner, et al., Long-term Climate Change: Projections, Commitments and Irreversibility, vol. 9781107057, 2013, https://doi.org/10.1017/CBO9781107415324.024.

[47] J. Cortekar, S. Bender, M. Brune, M. Groth, Why climate change adaptation in cities needs customised and flexible climate services, Clim. Serv. 4 (2016) 42–51, https://doi.org/10.1016/j.cliser.2016.11.002.

[48] Z.A. Alemu, M.O. Dioha, Climate change and trend analysis of temperature: the case of Addis Ababa, Ethiopia, Environ. Syst. Res. 9 (1) (2020), https://doi.org/10.1186/s40068-020-00190-5.

[49] L. Cochrane, P. Costolansk, Climate change vulnerability and adaptability in an urban context: a case study of Addis Ababa, Ethiopia, Int. J. Sociol. Anthropol. 5 (6) (2013) 192–204, https://doi.org/10.5897/ijsa2013.0459.

[50] J.A. Patz, D. Campbell-Lendrum, T. Holloway, J.A. Foley, Impact of regional climate change on human health, Nature 438 (7066) (2005) 310–317, https://doi.org/10.1038/nature04188.

[51] J. Tan, et al., The urban heat island and its impact on heat waves and human health in Shanghai, Int. J. Biometeorol. 54 (1) (2010) 75–84, https://doi.org/10.1007/s00484-009-0256-x.

[52] B.K. Arsiso, G.M. Tsidu, G.H. Stoffberg, T. Tadesse, "In fl uence of urbanization-driven land use/cover change on climate : the case of Addis Ababa, Ethiopia 105 (May 2017) (2018) 212–223, https://doi.org/10.1016/j.pce.2018.02.009.

[53] G. Feyissa, G. Zeleke, W. Bewket, E. Gebremariam, Downscaling of future temperature and precipitation extremes in Addis Ababa under climate change, Climate 6 (3) (2018), https://doi.org/10.3390/cli6030058.

[54] C. McSweeney, M. New, G. Lizcano, X. Lu, The UNDP climate change country profiles, Bull. Am. Meteorol. Soc. 91 (2) (2010) 157–166, https://doi.org/10.1175/2009BAMS2826.1.

[55] B.E. Feke, T. Terefe, K. Ture, D. Hunde, Variability and trends of observed minimum , maximum and average temperature over Northwestern parts of Ethiopia Since 1987, 2021 vol. 27.

[56] K.A. Elzopy, A.K. Chaturvedi, K.M. Chandran, G. Gopinath, K. Naveena, U. Surendran, Trend analysis of long-term rainfall and temperature data for Ethiopia, S. Afr. Geogr. J. 103 (3) (2021) 381–394, https://doi.org/10.1080/03736245.2020.1835699.

[57] 2007 National Meteorological Agency [NMA], The Federal Democratic Republic of Ethiopia Climate Change National Adaptation Programme of Action (NAPA) of Ethiopia Climate Change National Adaptation Programme of Action (Napa) of Ethiopia, no. June, 2007, p. 85 [Online]. Available: https://unfccc.int/resource/docs/napa/eth01.pdf.

[58] B.K. Arsiso, G. Mengistu Tsidu, G.H. Stoffberg, Signature of present and projected climate change at an urban scale: the case of Addis Ababa, Phys. Chem. Earth 105 (2018) 104–114, https://doi.org/10.1016/j.pce.2018.03.008.

[59] A.G. Berhe, D.B. Erena, I.M. Hassen, T.L. Mamaru, Y.A. Soressa, City profile: Addis Ababa, World Lit. Today 96 (3) (2017) 5, https://doi.org/10.1353/wlt.2022.0101.

[60] M. Wubneh, Addis Ababa, Ethiopia - africa's diplomatic capital, Cities 35 (2013) 255–269, https://doi.org/10.1016/j.cities.2013.08.002.

[61] UN-Habitat, Addis Ababa Urban Profile, 2008.

[62] E. Teferi, H. Abraha, Urban heat island effect of Addis Ababa city: implications of urban green spaces for climate change adaptation, Clim. Chang. Adapt. Africa (2017) 205–215, https://doi.org/10.1007/978-3-319-49520-0.

[63] H. Worku, Integrating Climate Change Adaptation Strategies in Urban Planning and Landscape Design of Addis Ababa City , Ethiopia Using Urban Planning and Landscape Design to Mitigate Flooding , Drought , and Urban Heat Island Effects, 2017, pp. 5–21, https://doi.org/10.1002/tqem.21514.

[64] G. Feyissa, G. Zeleke, E. Gebremariam, W. Bewket, GIS Based Quantification and Mapping of Climate Change Vulnerability Hotspots in Addis Ababa, 2018.

[65] D. Conway, C. Mould, W. Bewket, Over one century of rainfall and temperature observations in Addis Ababa, Ethiopia, Int. J. Climatol. 24 (1) (2004) 77–91, https://doi.org/10.1002/joc.989.

[66] T. Woldegerima, K. Yeshitela, S. Lindley, Characterizing the urban environment through urban morphology types (UMTs) mapping and land surface cover analysis: the case of Addis Ababa, Ethiopia, Urban Ecosyst. 20 (2) (2016) 245–263, https://doi.org/10.1007/s11252-016-0590-9.

[67] Addis Ababa City Planning Project Office, "Addis Ababa City Structure Plan," *Aacppo*, 2017, pp. 1–317 [Online]. Available: https://c40-production-images.s3.amazonaws.com.

[68] N.H. Koroso, Urban land policy and urban land use efficiency: an analysis based on remote sensing and institutional credibility thesis, Land Use Pol. 132 (May) (2023) 106827, https://doi.org/10.1016/j.landusepol.2023.106827.

[69] AAEP&GD, Addis Ababa City Climate Action Plan, vol. 149, 2021.

[70] D. Wanyama, A Spatial Analysis of Climate Change Effects on Maize Productivity in Kenya, 2017 [Online]. Available: https://ir.una.edu/gmt/1.

[71] IPCC, Climate Change 2007 Impacts, Adaptation and Vulnerability, 2007, https://doi.org/10.1016/B978-008044910-4.00250-9.

[72] WMO, Guidelines on the Definition and Characterization of Extreme Weather and Climate Events, vol. 1310, 2023.

[73] O. Huisman, R.A. de By, Principles of geographic information systems: an introductory textbook, J. Multivariate Anal. 127 (2009) 98–111, https://doi.org/10.1016/j.jmva.2014.02.006.

[74] S. Nandi, P. Patel, S. Swain, IMDLIB: an open-source library for retrieval, processing and spatiotemporal exploratory assessments of gridded meteorological observation datasets over India, Environ. Model. Software 171 (October 2023) (2024) 105869, https://doi.org/10.1016/j.envsoft.2023.105869.

[75] R.P. Haining, R. Kerry, M.A. Oliver, Geography , Spatial Data Analysis , and Geostatistics : an Overview, vol. 42, 2010, pp. 7–31.

[76] A.M. Mosammam, Geostatistics: modeling spatial uncertainty, second ed. J. Appl. Stat. 40 (4) (2013) 923, https://doi.org/10.1080/02664763.2012.750474.

[77] J.S. Yang, Y.Q. Wang, P. V August, Estimation of Land Surface Temperature Using Spatial Interpolation and Satellite-Derived Surface Emissivity, 2004, pp. 89–96.

[78] H. Apaydin, F. Kemal Sonmez, Y.E. Yildirim, Spatial interpolation techniques for climate data in the GAP region in Turkey, Clim. Res. 28 (1) (2013) 31–40, https://doi.org/10.3354/cr028031.

[79] D. Ozturk, F. Kilic, Geostatistical Approach for Spatial Interpolation of Meteorological Data, 2016, pp. 2121–2136, vol. 88.

[80] Y. Xiao, et al., Geostatistical interpolation model selection based on ArcGIS and spatio-temporal variability analysis of groundwater level in piedmont plains, northwest China, SpringerPlus 5 (1) (2016), https://doi.org/10.1186/s40064-016-2073-0.

[81] Y. Hou, X. Huang, L. Zhao, Point-to-Surface upscaling algorithms for snow depth ground observations, Rem. Sens. 14 (19) (2022), https://doi.org/10.3390/rs14194840.

[82] Y. Yuan, et al., Effect of normalization methods on accuracy of estimating low- and high-molecular weight PAHs distribution in the soils of a coking plant, Int. J. Environ. Res. Publ. Health 19 (23) (2022), https://doi.org/10.3390/ijerph192315470.

[83] D.L. Phillips, J. Dolph, D. Marks, A comparison of geostatistical procedures for spatial analysis of precipitation in mountainous terrain *, 1992, pp. 119–141, vol. 58.

[84] M. Ashraf, J.C. Loftis, K.G. Hubbard, Application of geostatistics to evaluate partial weather station networks, 1997 vol. 1923, no. 1973.

[85] Z. Chuanyan, N. Zhongren, C. Guodong, Methods for modelling of temporal and spatial distribution of air temperature at landscape scale in the southern Qilian mountains , China, 2005, pp. 209–220, https://doi.org/10.1016/j.ecolmodel.2005.03.016, vol. 189.

[86] J.D. Michaud, Spatial and Elevational Variations of Summer Rainfall in the Southwestern United Stated, 1995.

[87] P. Biernacik, W. Kazimierski, M. Włodarczyk-Sielicka, Comparative analysis of selected geostatistical methods for bottom surface modeling, Sensors 23 (8) (2023), https://doi.org/10.3390/s23083941.

[88] I. Piri, A. Khanamani, S. Shojaei, H. Fathizad, "Determination of the Best Geostatistical Method for Climatic Zoning in Iran Determination of the Best Geostatistical Method for Climatic Zoning in Iran,", November, 2016, https://doi.org/10.15666/aeer/1501.

[89] J.E. Joseph, et al., The Usefulness of Gridded Climate Data Products in Characterizing Climate Variability and Assessing Crop Production the Usefulness of Gridded Climate Data Products in Characterizing Climate Variability and Assessing Crop Production, 2020.

[90] T. Dinku, P. Ceccato, E. Grover-Kopec, M. Lemma, S.J. Corner, C.F. Ropelewski, Validation of satellite rainfall products over East Africa ' s complex topography, 2007, pp. 1503–1526, https://doi.org/10.1080/01431160600954688, vol. 28, no. 7.

[91] T. Dinku, et al., Bridging critical gaps in climate services and applications in africa, Earth Perspect 1 (1) (2014) 15, https://doi.org/10.1186/2194-6434-1-15.

[92] I. Ahmed, et al., Climate change impacts and adaptation strategies for agronomic crops, Clim. Chang. Agric (June) (2019), https://doi.org/10.5772/intechopen.82697.

[93] P. Frich, et al., Observed coherent changes in climatic extremes during the second half of the twentieth century, Clim. Res. 19 (3) (2002) 193–212, https://doi.org/10.3354/cr019193.

[94] J. Hofierka, H. Mitasova, J. Parajka, L. Mitas, Multivariate Interpolation of Precipitation Using Regularized Spline with Tension, 2002 vol. 6, no. 2.

[95] A. Asfaw, B. Simane, A. Hassen, A. Bantider, Variability and time series trend analysis of rainfall and temperature in northcentral Ethiopia: a case study in Woleka sub-basin, Weather Clim. Extrem. 19 (December 2017) (2018) 29–41, https://doi.org/10.1016/j.wace.2017.12.002.

[96] M.G. Donat, et al., Updated analyses of temperature and precipitation extreme indices since the beginning of the twentieth century: the HadEX2 dataset, J. Geophys. Res. Atmos. 118 (5) (2013) 2098–2118, https://doi.org/10.1002/jgrd.50150.

[97] Q. Guo, Z. He, Z. Wang, Simulating daily PM2.5 concentrations using wavelet analysis and artificial neural network with remote sensing and surface observation data, Chemosphere 340 (August) (2023) 139886, https://doi.org/10.1016/j.chemosphere.2023.139886.

[98] S. Mulugeta, C. Fedler, M. Ayana, Analysis of long-term trends of annual and seasonal rainfall in the Awash River Basin, Ethiopia, Water (Switzerland) 11 (7) (2019), https://doi.org/10.3390/w11071498.

[99] J.M. Collins, Temperature variability over africa, J. Clim. 24 (14) (2011) 3649–3666, https://doi.org/10.1175/2011JCLI3753.1.

[100] N. Wagesho, N.K. Goel, M.K. Jain, Variabilité temporelle et spatiale des précipitations annuelles et saisonnières sur l'Ethiopie, Hydrol. Sci. J. 58 (2) (2013) 354–373, https://doi.org/10.1080/02626667.2012.754543.

[101] S.M. Pingale, D. Khare, M.K. Jat, J. Adamowski, Trend analysis of climatic variables in an arid and semi-arid region of the Ajmer District, Rajasthan, India, J. Water Land Dev. 28 (1) (2016) 3–18, https://doi.org/10.1515/jwld-2016-0001.

[102] S. Addisu, Y.G. Selassie, G. Fissha, B. Gedif, Time series trend analysis of temperature and rainfall in lake Tana Sub-basin, Ethiopia, Environ. Syst. Res. 4 (1) (2015), https://doi.org/10.1186/s40068-015-0051-0.

[103] H. Apaydin, F. Kemal Sonmez, Y.E. Yildirim, Spatial interpolation techniques for climate data in the GAP region in Turkey, Clim. Res. 28 (1) (2004) 31–40, https://doi.org/10.3354/cr028031.

[104] S. Ly, C. Charles, A. Degré, Geostatistical interpolation of daily rainfall at catchment scale: the use of several variogram models in the Ourthe and Ambleve catchments, Belgium, Hydrol. Earth Syst. Sci. 15 (7) (2011) 2259–2274, https://doi.org/10.5194/hess-15-2259-2011.

[105] R. Sluiter, K. Nederlands, M. Instituut, Interpolation Methods for Climate Data Literature Review, August, 2014.

[106] W. Yue, J. Xu, H. Liao, L. Xu, Applications of spatial interpolation for climate variables based on geostatistics: a case study in gansu province, China, Geo Inf. Sci. 9 (1–2) (2003) 71–77, https://doi.org/10.1080/10824000309480590.

[107] B.V. Srinivasan, R. Duraiswami, R. Murtugudde, Efficient kriging for real-time spatio-temporal interpolation Linear kriging, 20th Conf. Probablility Stat. Atmos. Sci. (January 2015) (2010) 228–235.

[108] M.A. Oliver, R. Webster, Kriging: a method of interpolation for geographical information systems, Int. J. Geogr. Inf. Syst. 4 (3) (1990) 313–332, https://doi.org/10.1080/02693799008941549.

[109] P.F. Kuo, T.E. Huang, I.G.B. Putra, Comparing kriging estimators using weather station data and local greenhouse sensors, Sensors 21 (5) (2021) 1–15, https://doi.org/10.3390/s21051853.

[110] F.J. Moral, Comparison of different geostatistical approaches to map climate variables: application to precipitation, Int. J. Climatol. 30 (4) (2010) 620–631, https://doi.org/10.1002/joc.1913.

[111] M.R. Holdaway, Spatial modeling and interpolation of monthly temperature using kriging, Clim. Res. 6 (3) (1996) 215–225, https://doi.org/10.3354/cr006215.

[112] J. Ryu, M. Kim, K.-J. Cha, T.H. Lee, D.-H. Choi, Kriging Interpolation Methods in Geostatistics and DACE Model, 2002, pp. 619–632, vol. 16, no. 5.

[113] P. Goovaerts, Determining molecular weight distribution index from flow curves for polypropylene, J. Hydrol. 228 (3) (2000) 113–129.

[114] C. Li, Z. Lu, T. Ma, X. Zhu, A simple kriging method incorporating multiscale measurements in geochemical survey, J. Geochem. Explor. 101 (2) (2009) 147–154, https://doi.org/10.1016/j.gexplo.2008.06.003.

[115] R. Sluiter, Interpolation methods for climate data literature review, no. August, Intern (2009), 2009–4.

[116] T. Appelhans, E. Mwangomo, D.R. Hardy, A. Hemp, T. Nauss, Evaluating machine learning approaches for the interpolation of monthly air temperature at Mt. Kilimanjaro, Tanzania, Spat. Stat. 14 (2015) 91–113, https://doi.org/10.1016/j.spasta.2015.05.008.

[117] M. Borga, A. Vizzaccaro, On the interpolation of hydrologic variables: Formal equivalence of multiquadratic surface fitting and kriging, J. Hydrol. 195 (1–4) (1997) 160–171, https://doi.org/10.1016/S0022-1694(96)03250-7.

[118] M.R. Holdaway, M.R. Holdaway, Spatial modeling and interpolation of mont temperature using kriging, 1996, pp. 215–225, vol. 6, no. 3.

[119] J. Li, A.D. Heap, A review of spatial interpolation methods for environmental scientists, GeoCat# 68, Aust. Geol. Surv. Organ. (2008/23) (2008) 154, http://www.ga.gov.au/image_cache/GA12526.pdf.

[120] M.K. Zegeye, K.T. Bekitie, D.N. Hailu, Spatio - temporal variability and trends of hydroclimatic variables at zarima sub - basin north western Ethiopia, Environ. Syst. Res. 5 (2022), https://doi.org/10.1186/s40068-022-00273-5.

[121] F.K. Muthoni, et al., Long-term spatial-temporal trends and variability of rainfall over Eastern and Southern Africa, Theor. Appl. Climatol. 137 (3–4) (2019) 1869–1882, https://doi.org/10.1007/s00704-018-2712-1.

[122] M.M. Alemu, G.T. Bawoke, Analysis of spatial variability and temporal trends of rainfall in Amhara Region, Ethiopia, J. Water Clim. Chang. 11 (4) (2020) 1505–1520, https://doi.org/10.2166/wcc.2019.084.

[123] A. Alemayehu, M. Maru, W. Bewket, M. Assen, Spatiotemporal variability and trends in rainfall and temperature in Alwero watershed, western Ethiopia, Environ. Syst. Res. 9 (1) (2020), https://doi.org/10.1186/s40068-020-00184-3.

[124] G. Bayable, G. Amare, G. Alemu, T. Gashaw, Spatiotemporal variability and trends of rainfall and its association with pacific ocean sea surface temperature in west harerge zone, eastern Ethiopia, Environ. Syst. Res. 10 (1) (2021), https://doi.org/10.1186/s40068-020-00216-y.

[125] M. Eshetu, Hydro-climatic variability and trend analysis of modjo river watershed, awash river basin of Ethiopia, J. Environ. Earth Sci. 11 (Figure 1) (2021) 1–8, https://doi.org/10.7176/jees/11-9-04.

[126] W. Hare, Assessment of Knowledge on Impacts of Climate Change – Contribution to the Specification of Art. 2 of the UNFCCC, 1, 2003 [Online]. Available: http://www.wbgu.de/wbgu_sn2003_ex01.pdf.

[127] C.T. Agnew, A. Chappell, Drought in the sahel, Black Scholar 5 (10) (2000) 37–42, https://doi.org/10.1080/00064246.1974.11431441.

[128] H. Chen, S. Guo, C. yu Xu, V.P. Singh, Historical temporal trends of hydro-climatic variables and runoff response to climate variability and their relevance in water resource management in the Hanjiang basin, J. Hydrol. 344 (3–4) (2007) 171–184, https://doi.org/10.1016/j.jhydrol.2007.06.034.

[129] Y.A. Orke, M.H. Li, Hydroclimatic variability in the bilate watershed, Ethiopia, Climate 9 (6) (2021), https://doi.org/10.3390/cli9060098.

[130] Z.W. Kundzewicz, M. Radziejewski, Methodologies for Trend Detection, November, 2006, pp. 538–550.

[131] S. Sahoo, S. Swain, A. Goswami, R. Sharma, B. Pateriya, Assessment of trends and multi-decadal changes in groundwater level in parts of the Malwa region, Punjab, India, Groundw. Sustain. Dev. 14 (October 2020) (2021) 100644, https://doi.org/10.1016/j.gsd.2021.100644.

[132] P. Sonali, D. Nagesh Kumar, Review of trend detection methods and their application to detect temperature changes in India, J. Hydrol. 476 (2013) 212–227, https://doi.org/10.1016/j.jhydrol.2012.10.034.

[133] K.H. Hamed, A.R. Rao, A modified Mann-Kendall trend test for autocorrelated data, J. Hydrol. 36 (15_suppl) (1998), https://doi.org/10.1200/jco.2018.36.15_suppl.522, 522–522.

[134] D. Duhan, A. Pandey, K.P.S. Gahalaut, R.P. Pandey, Spatial and temporal variability in maximum, minimum and mean air temperatures at Madhya Pradesh in central India, Compt. Rendus Geosci. 345 (1) (2013) 3–21, https://doi.org/10.1016/j.crte.2012.10.016.

[135] S. Suryavanshi, A. Pandey, U.C. Chaube, N. Joshi, Long-term historic changes in climatic variables of Betwa Basin, India, Theor. Appl. Climatol. 117 (3–4) (2014) 403–418, https://doi.org/10.1007/s00704-013-1013-y.

[136] T.G. Gebremicael, Y.A. Mohamed, P.V. Zaag, E.Y. Hagos, Temporal and spatial changes of rainfall and streamflow in the Upper Tekezē-Atbara river basin, Ethiopia, Hydrol. Earth Syst. Sci. 21 (4) (2017) 2127–2142, https://doi.org/10.5194/hess-21-2127-2017.

[137] G. Kiros, A. Shetty, L. Nandagiri, Analysis of variability and trends in rainfall over northern Ethiopia, Arabian J. Geosci. 9 (6) (2016), https://doi.org/10.1007/s12517-016-2471-1.

[138] Y. Mohammed, F. Yimer, M. Tadesse, K. Tesfaye, Variability and trends of rainfall extreme events in north east highlands of Ethiopia, Int. J. Hydrol. 2 (5) (2018) 594–605, https://doi.org/10.15406/ijh.2018.02.00131.

[139] C. Ngongondo, C.Y. Xu, L. Gottschalk, B. Alemaw, Evaluation of spatial and temporal characteristics of rainfall in Malawi: a case of data scarce region, Theor. Appl. Climatol. 106 (1–2) (2011) 79–93, https://doi.org/10.1007/s00704-011-0413-0.

[140] S. Swain, S.K. Mishra, A. Pandey, D. Dayal, Assessment of drought trends and variabilities over the agriculture-dominated Marathwada Region, India, Environ. Monit. Assess. 194 (12) (2022), https://doi.org/10.1007/s10661-022-10532-8.

[141] H.B. Mann, "Non-Parametric test against trend,", Econometrica 13 (3) (1945) 245–259 [Online]. Available: http://www.economist.com/node/18330371? story%7B_%7Did=18330371.

[142] C.S. Signorino, J.M. Ritter, Tau-b or not Tau-b: measuring the similarity of foreign policy positions, Int. Stud. Q. 43 (1) (1999) 115–144, https://doi.org/ 10.1111/0020-8833.00113.

[143] F. Wang, et al., Re-Evaluation of the power of the mann-kendall test for detecting monotonic trends in hydrometeorological time series, Front. Earth Sci. 8 (February) (2020) 1–12, https://doi.org/10.3389/feart.2020.00014.

[144] S. Yue, P. Pilon, G. Cavadias, Power of the Mann ± Kendall and Spearman ' S Rho Tests for Detecting Monotonic Trends in Hydrological Series, vol. 259, 2002, pp. 254–271.

[145] Q. Zhang, J. Li, Y.D. Chen, X. Chen, Observed changes of temperature extremes during 1960-2005 in China: natural or human-induced variations? Theor. Appl. Climatol. 106 (3–4) (2011) 417–431, https://doi.org/10.1007/s00704-011-0447-3.

[146] S. Swain, S.K. Mishra, A. Pandey, D. Dayal, Spatiotemporal assessment of precipitation variability, seasonality, and extreme characteristics over a Himalayan catchment, Theor. Appl. Climatol. 147 (1–2) (2022) 817–833, https://doi.org/10.1007/s00704-021-03861-0.

[147] S. Swain, S.K. Mishra, A. Pandey, Assessing spatiotemporal variation in drought characteristics and their dependence on timescales over Vidarbha Region, India, Geocarto Int. 37 (27) (2022) 17971–17993, https://doi.org/10.1080/10106049.2022.2136260.

[148] S. Swain, S.K. Mishra, A. Pandey, A detailed assessment of meteorological drought characteristics using simplified rainfall index over Narmada River Basin, India, Environ. Earth Sci. 80 (6) (2021) 1–15, https://doi.org/10.1007/s12665-021-09523-8.

[149] K.H. Ahn, V. Merwade, Quantifying the relative impact of climate and human activities on streamflow, J. Hydrol. 515 (April) (2014) 257–266, https://doi.org/ 10.1016/j.jhydrol.2014.04.062.

[150] P.K. Sen, Estimates of the regression coefficient based on Kendall's tau, J. Am. Stat. Assoc. 63 (324) (1968) 1379–1389, https://doi.org/10.1080/ 01621459.1968.10480934.

[151] R. Bouza-Deaño, M. Ternero-Rodríguez, A.J. Fernández-Espinosa, Trend study and assessment of surface water quality in the Ebro River (Spain), J. Hydrol. 361 (3–4) (2008) 227–239, https://doi.org/10.1016/j.jhydrol.2008.07.048.

[152] A.A. Mekonen, A.B. Berlie, M.B. Ferede, Spatial and temporal drought incidence analysis in the northeastern highlands of Ethiopia, Geoenvironmental Disasters 7 (1) (2020), https://doi.org/10.1186/s40677-020-0146-4.

[153] S. Ray, S.S. Das, P. Mishra, A.M.G. Al Khatib, Time series SARIMA modelling and forecasting of monthly rainfall and temperature in the south asian countries, Earth Syst. Environ. 5 (3) (2021) 531–546, https://doi.org/10.1007/s41748-021-00228-3.

[154] S.K. Jain, V. Kumar, Trend analysis of rainfall and temperature data for India, Curr. Sci. 102 (1) (2012) 37–49.

[155] S. Agarwal, A.S. Suchithra, S.P. Singh, Analysis and interpretation of rainfall trend using Mann-Kendall's and Sen's slope Method, Indian J. Ecol. 48 (2) (2021) 453–457.

[156] F.T. Gelata, H. Jiqin, S. Chaka Gemeda, Application of MK trend and test of Sen's slope estimator to measure impact of climate change on the adoption of conservation agriculture in Ethiopia, J. Water Clim. Chang. 14 (3) (2023) 977–988, https://doi.org/10.2166/wcc.2023.508.

[157] T.M. Weldegerima, T.T. Zeleke, B.S. Birhanu, B.F. Zaitchik, Z.A. Fetene, Analysis of rainfall trends and its relationship with SST signals in the lake tana basin , Ethiopia, 2018 vol. 2018.

[158] B.F. Frimpong, A. Koranteng, F. Molkenthin, Analysis of temperature variability utilising Mann–Kendall and Sen's slope estimator tests in the Accra and Kumasi Metropolises in Ghana, Environ. Syst. Res. 11 (1) (2022) 1–13, https://doi.org/10.1186/s40068-022-00269-1.

[159] I.T. Jollife, J. Cadima, Principal component analysis: a review and recent developments, Philos. Trans. R. Soc. A Math. Phys. Eng. Sci. 374 (2065) (2016), https://doi.org/10.1098/rsta.2015.0202.

[160] S. Swain, S. Sahoo, A.K. Taloor, Groundwater quality assessment using geospatial and statistical approaches over Faridabad and Gurgaon districts of National Capital Region, India, Appl. Water Sci. 12 (4) (2022) 1–14, https://doi.org/10.1007/s13201-022-01604-8.

[161] Z. Ling, Y. Gao, Q. Chen, Application of principal component analysis in meteorological forecast, IOP Conf. Ser. Earth Environ. Sci. 631 (1) (2021), https://doi. org/10.1088/1755-1315/631/1/012019.

[162] Z. Zuśka, J. Kopcińska, E. Dacewicz, B. Skowera, J. Wojkowski, A. Ziernicka-Wojtaszek, Application of the principal component analysis (PCA) method to assess the impact of meteorological elements on concentrations of particulate matter (PM10): a case study of the mountain valley (the Sacz Basin, Poland), Sustain. Times 11 (23) (2019) 1–12, https://doi.org/10.3390/su11236740.

[163] P.D. Kilmer, Review article: review article, Journalism 11 (3) (2010) 369–373, https://doi.org/10.1177/1461444810365020.

[164] M.B. Richman, P.J. Lamb, Climatic pattern analysis of three- and seven-day summer rainfall in the central United States: some methodological considerations and a regionalization, J. Clim. Appl. Meteorol. 24 (12) (1985) 1325–1343, https://doi.org/10.1175/1520-0450(1985)024<1325:CPAOTA>2.0.CO;2.

[165] L. Tadić, O. Bonacci, T. Brleković, An example of principal component analysis application on climate change assessment, Theor. Appl. Climatol. 138 (1–2) (2019) 1049–1062, https://doi.org/10.1007/s00704-019-02887-9.

[166] D.B. Reusch, R.B. Alley, B.C. Hewitson, Relative performance of self-organizing maps and principal component analysis in pattern extraction from synthetic climatological data, Polar Geogr. 29 (3) (2005) 188–212, https://doi.org/10.1080/789610199.

[167] P.A. Mayewski, et al., Major features and forcing of high-latitude northern hemisphere atmospheric circulation using a 110,000-year-long glaciochemical series, J. Geophys. Res. Ocean. 102 (C12) (1997) 26345–26366, https://doi.org/10.1029/96JC03365.

[168] J.E. Walsh, Temporal and Spatial Scales of the Arctic Circulation, 1978.

[169] T.A. Bahita, S. Swain, P. Pandey, A. Pandey, Assessment of heavy metal contamination in livestock drinking water of Upper Ganga Canal (Roorkee City, India), Arabian J. Geosci. 14 (24) (2021) 1–13, https://doi.org/10.1007/s12517-021-08874-7.

[170] D. Yang, D. Dong, L.H.I. Lim, L. Liu, Analyzing big time series data in solar engineering using features and PCA, Sol. Energy 153 (2017) 317–328, https://doi. org/10.1016/j.solener.2017.05.072.

[171] W. Zgłobicki, M. Telecka, S. Skupiński, A. Pasierbińska, M. Kozieł, Assessment of heavy metal contamination levels of street dust in the city of Lublin, E Poland, Environ. Earth Sci. 77 (23) (2018) 1–11, https://doi.org/10.1007/s12665-018-7969-2.

[172] K.R. Gabriel, The Biplot display of multivariate matrices with application to principal components analysis, Biometrika 58 (1971) 453–467.

[173] M.B. Richman, Obliquely Rotatted Principal Components: an Improved Meteorological Map Typing Technique?, 1981.

[174] M. Asefa, M. Cao, Y. He, E. Mekonnen, X. Song, J. Yang, Ethiopian vegetation types, climate and topography, Plant Divers 42 (4) (2020) 302–311, https://doi. org/10.1016/j.pld.2020.04.004.

[175] AACPPO, Addis Ababa City Structure Plan, Aacppo, 2017, pp. 1–10.

[176] W. Legese, D K, K. T, Perception of farmers on climate change and their adaptive strategies over bale highlands, southeastern Ethiopia, J. Earth Sci. Climatic Change 9 (9) (2018), https://doi.org/10.4172/2157-7617.1000491.

[177] A. Alemayehu, W. Bewket, Local spatiotemporal variability and trends in rainfall and temperature in the central highlands of Ethiopia, Geogr. Ann. Ser. A Phys. Geogr. 99 (2) (2017) 85–101, https://doi.org/10.1080/04353676.2017.1289460.

[178] A. Berhane, G. Hadgu, W. Worku, B. Abrha, Trends in extreme temperature and rainfall indices in the semi-arid areas of Western Tigray, Ethiopia, Environ. Syst. Res. 9 (1) (2020), https://doi.org/10.1186/s40068-020-00165-6.

[179] F. Benti, M. Abara, Trend analyses of temperature and rainfall and their response to global CO2 emission in masha, southern Ethiopia, Caraka Tani J. Sustain. Agric. 34 (1) (2019) 67, https://doi.org/10.20961/carakatani.v34i1.28022.

[180] A. Belay, et al., Analysis of climate variability and trends in Southern Ethiopia, Climate 9 (6) (2021) 1–17, https://doi.org/10.3390/cli9060096.

[181] B. Getachew, Trend analysis of temperature and rainfall in south gonder zone, anhara Ethiopia, J. Degrad. Min. Lands Manag. 5 (2) (2018) 1111–1125, https:// doi.org/10.15243/jdmlm.2018.052.1111.

[182] K. Pandžić, M. Kisegi, Principal Component analysis of a local temperature field within the global circulation, Theor. Appl. Climatol. 41 (4) (1990) 177–200, https://doi.org/10.1007/BF00866450.

[183] IPCC, Climate Change 2023: Synthesis Report: Summary for Policy Makers, 2023 [Online]. Available: https://www.unep.org/resources/report/climate-change-2023-synthesis-report.

[184] C. Mcsweeney, M. New, G. Lizcano, UNDP climate change country profiles: Ethiopian, Available:1–18., pp. 1–27, http://country-profiles.geog.ox.ac.uk/, 2008. (Accessed 10 May 2013).

[185] C.H. Trisos, et al., Climate Change 2022: Impacts, Adaptation and Vulnerability, 2022, https://doi.org/10.1017/9781009325844.011.1286 vol. 1.

[186] G.C. Guptha, S. Swain, N. Al-Ansari, A.K. Taloor, D. Dayal, Evaluation of an urban drainage system and its resilience using remote sensing and GIS, Remote Sens. Appl. Soc. Environ. 23 (May) (2021) 100601, https://doi.org/10.1016/j.rsase.2021.100601.

[187] United Nations, The Sustainable Development Goals Report 2019, United Nations Publ. issued by Dep. Econ. Soc. Aff., 2022, p. 64 [Online]. Available: https://unstats.un.org/sdgs/report/2022/%0A.

[188] D. Gatarić, M. Belij, B. Đerčan, D. Filipović, The origin and development of Garden cities: an overview, Zb. Rad. - Geogr. Fak. Univ. u Beogradu (2019) 33–43, https://doi.org/10.5937/zrgfub1901033g, no. 67–1.